

^{89}Y NMR probe of Zn induced local magnetism in $\text{YBa}_2(\text{Cu}_{1-y}\text{Zn}_y)_3\text{O}_{6+x}$

A.V. Mahajan^{1,a}, H. Alloul¹, G. Collin², and J.F. Marucco³

¹ Laboratoire de Physique des Solides^b, Université Paris-Sud, 91405 Orsay Cedex, France

² LLB, CE Saclay, CEA-CNRS, 91191, Gif-sur-Yvette, France

³ Laboratoire des Composés Non-Stoichiométriques, Université Paris-Sud, 91405 Orsay Cedex, France

Received 11 March 1999

Abstract. We present detailed data and analysis of the effects of Zn substitution on the planar Cu site in $\text{YBa}_2\text{Cu}_3\text{O}_{6+x}$ (YBCO_{6+x}) as evidenced from our ^{89}Y NMR measurements on oriented powders. For $x \ll 1$ we find additional NMR lines which are associated with the Zn substitution. From our data on the intensities and temperature dependence of the shift, width, and spin-lattice relaxation rate of these resonances, we conclude that the spinless Zn $3d^{10}$ state induces local moments on the near-neighbour (nn) Cu atoms. Additionally, we conjecture that the local moments actually extend to the farther Cu atoms with the magnetization alternating in sign at subsequent nn sites. We show that this analysis is compatible with ESR data taken on dilute Gd doped (on the Y site) and on neutron scattering data reported recently on Zn substituted YBCO_{6+x} . For optimally doped compounds ^{89}Y nn resonances are not detected, but a large T -dependent contribution to the ^{89}Y NMR linewidth is evidenced and is also attributed to the occurrence of a weak induced local moment near the Zn. These results are compatible with macroscopic magnetic measurements performed on YBCO_{6+x} samples prepared specifically in order to minimize the content of impurity phases. We find significant differences between the present results on the underdoped YBCO_{6+x} samples and ^{27}Al NMR data taken on Al^{3+} substituted on the Cu site in optimally doped La_2CuO_4 . Further experimental work is needed to clarify the detailed evolution of the impurity induced magnetism with hole content in the cuprates.

PACS. 74.72.Bk Y-based cuprates – 74.25.Ha Magnetic properties – 76.60.Cq Chemical and Knight shifts

1 Introduction

It is now experimentally well-established that the CuO_2 planes are responsible for the magnetic and superconducting properties of the cuprates. However the interconnection between these two properties is still an essential but unanswered question. Understanding the normal state of the cuprates is still a prerequisite for any theoretical approach to the microscopic origin of High Temperature Superconductivity. In the recent past, considerable interest has been aroused due to the detection of a pseudo-gap in the spin excitation spectrum of the cuprates for underdoped materials (the word pseudo is prefixed because although a strong decrease in the intensity of excited states is detected well above the superconducting transition temperature T_c , a real gap is only detected below T_c). The first indications of a pseudo-gap were provided in the microscopic NMR measurements of the susceptibil-

ity of the CuO_2 planes. ^{89}Y NMR shifts in YBCO_{6+x} of Alloul *et al.* [1] were found to decrease markedly with decreasing T . The large decrease of the static susceptibility was interpreted to be due to an opening of a pseudo-gap in the homogeneous $\mathbf{q} = 0$ excitations of the system. In the underdoped ($x < 1$ for YBCO_{6+x}) high- T_c cuprates, a similar decrease of the spin-lattice relaxation rate ^{63}Cu $1/T_1T$ [2], which is dominated by the imaginary part of the susceptibility at the AF wave vector $\mathbf{q} = (\pi, \pi)$ was also indicative of a pseudo-gap in the spin excitations at this wave vector [3].

The inelastic neutron scattering experiments which followed [4,5], clearly confirmed the existence of this pseudo spin-gap at (π, π) , and allowed measurements of the frequency dependence of the excitations. The temperatures at which these two pseudo-gaps begin to open are found to be different, and it is not clear at present whether they signal different cross-overs between distinct states or a single cross-over phenomenon. The latter case would imply a wave-vector dependence of the pseudo-gap. Presently, the existence of a pseudogap for the underdoped high- T_c superconductors has been detected by many techniques

^a Permanent address: Indian Institute of Technology, Powai, Bombay 400 076, India

e-mail: mahajan@phy.iitb.ernet.in

^b URA 2 CNRS

such as transport, photoemission, etc. While various explanations are proposed for the pseudo-gaps, it is believed that the essential physics of the normal state (and perhaps the superconducting state), of the cuprates might be linked to it.

In order to better characterise the properties of the cuprates it has appeared quite important to understand their modifications due to impurities or disorder. Atomic substitutions on the planar Cu site are naturally found to be the most detrimental to superconductivity, while modification in the charge reservoir chains mainly yield changes in hole doping. For such studies the YBCO_{6+x} system is particularly suitable, as the variation of impurity induced magnetism with hole doping can be studied by merely changing the oxygen content x for a given impurity content. In classical superconductors, T_c is mainly affected by magnetic impurity substitutions. In cuprates it has been shown that even a non-magnetic impurity like Zn ($3d^{10}$), which substitutes on the Cu site of the CuO₂ plane strongly decreases the superconducting transition temperature T_c (about 10.6 K/% Zn for $x = 1$). It has also been anticipated [6] and then shown experimentally that although Zn itself is non-magnetic, it induces a modification of the magnetic properties of the correlated spin system of the CuO₂ planes [7]. Using ⁸⁹Y NMR we have further shown, in the preliminary report of the present work [8], that local magnetic moments are induced on the nn Cu of the Zn substituent in the CuO₂ plane. Two important results have been demonstrated:

- i) the $q = 0$ pseudo-gap was found unaffected by Zn even when T_c is reduced to zero for YBCO_{6.6};
- ii) the magnitude of the induced local moment is strongly dependent on the carrier concentration [9].

Since our reports, other experimental evidence by NMR in YBCO [10,11], in YBa₂Cu₄O₈ (1248) [12], in La₂CuO₄ [13], or ESR in YBCO and 1248 [14], have confirmed that the occurrence of local moment induced by non-magnetic impurities on the Cu sites is a general property of cuprates. The local moments have been observed as well in macroscopic bulk susceptibility data [9,15–17]. The Zn-induced modifications of the magnetic excitations both in the superconducting and the normal state have been studied by neutron scattering [18,19]. Also, electrical transport [20,21], and thermal properties [22] of substituted high- T_c cuprates have been investigated.

However some studies have concluded that the susceptibility near the Zn does not exhibit a Curie behaviour, at least for $x = 1$, or that the AF correlations were destroyed in the vicinity of the Zn substituents [14,23]. Also some data have been interpreted as due to the total disappearance of the pseudo-gap in the vicinity of Zn. Finally, the dynamics of the local moment [13] appears to be quite different in La₂CuO₄:Al than in our results.

To clarify the situation, we present in this article an extended report of our experimental data, and perform an exhaustive comparison with the literature. We examine in detail the effect of Zn on ⁸⁹Y NMR, in oriented powders of YBCO_{6+x}:Zn _{y} with $0.5\% \leq y \leq 4\%$, for $x = 0.64$ and 1. NMR, being a local probe, provides use-

ful information about the impurity induced short-range and long-range effects in the metal *via* an analysis of the lineshape, Knight shift, and linewidth. In Section 2, we present the experimental details regarding sample preparation and the procedures adopted for NMR measurements. In Section 3, a thorough description of the results of our NMR work, allows us to highlight the differences in the effect of Zn doping in underdoped and overdoped YBCO. In Section 4, the NMR shift, linewidth, and relaxation rate data are analyzed considering Zn induced local moments on the neighbouring Cu. A contrasting comparison with the other experimental results introduced in this section is contained in the last subsection of 4. In the conclusion section we summarize our overall view of the experimental situation, and discuss several theoretical works which have paid some attention to the induced magnetism in cuprates.

2 Experimental details

Samples of YBCO_{6+x}:Zn were prepared by conventional solid state reaction techniques as described elsewhere [24]. Large (single crystal) grain (size > 50 microns) samples were made which were finely ground before oxygenation (see Ref. [25] for further details regarding characterisation). In order to prepare the samples with maximum oxygen content, oxygenation was done at ~ 300 °C for a long period (> 10 days) which ensured homogeneity of oxygen content. For preparing samples with a reduced oxygen content, the maximally oxidized samples were treated in vacuum in a thermobalance at variable temperatures, up to 450 °C. The samples were quenched to room temperature when the equilibrium oxygen content was reached.

In the case of YBCO_{6+x} (without Zn), when the maximum oxidized samples were deoxidized to a point where the sample decomposed, the weight loss corresponded to $\delta x (= x_{\max} - x_{\min}) = 1.0$. However, on addition of Zn, the actual maximum value of δx which could be reached, progressively decreases and equals 0.92 for 4% Zn. Since for the Zn doped samples, the ortho-tetra structural phase transition still takes place for an oxygen content of $x_{\min} + 0.45$ (as in YBCO_{6+x} without Zn) [26], it appears that $x_{\min} = 6.0$ in the Zn doped samples while x_{\max} linearly decreases from 7.0 for 0% Zn to 6.92 for 4% Zn. These samples with specific oxygen and zinc contents were then fixed in Stycast 1266 and cured overnight in a field of 7.5 Tesla in order to orient the grains with the c axis aligned along the applied field direction.

NMR measurements were performed by standard pulsed NMR techniques. We observed the spin echos after a $\pi/2 - \pi$ sequence followed by a $3\pi/2 - \pi$ sequence. A perfect inversion of the spin-echo in the latter relative to the first sequence ensured the correctness of the $\pi/2$ pulse length (about 13 μ s at room temperature). The ⁸⁹Y shift was measured with respect to a standard YCl₃ solution.

The ⁸⁹Y spin-lattice relaxation time T_1 was determined using a $\pi/2 - \pi$ sequence, with a repetition time t_{rep} . An exponential fit of the nuclear magnetization (obtained from a Fourier Transform, FT, of the time domain

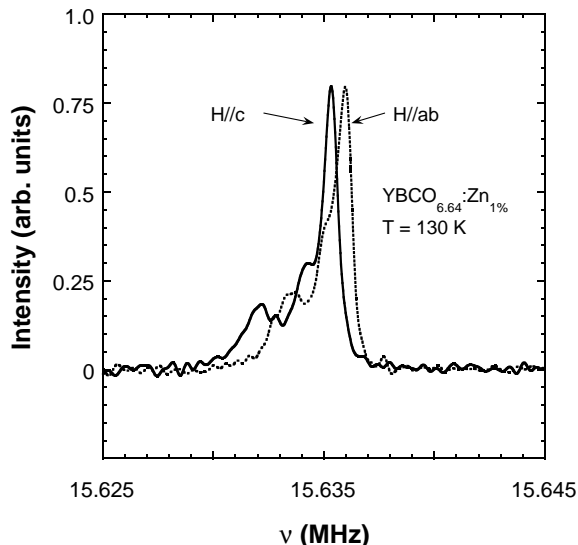


Fig. 1. ^{89}Y NMR lineshape at 130 K in $\text{YBCO}_{6.64}:\text{Zn}_{1\%}$ when the duty cycle of the pulse sequence, t_{rep} , is 20 s, with the sample c axis aligned parallel or perpendicular to the applied field. The relative intensity of the nn lines is enhanced here, since they have a T_1 comparable to t_{rep} while the mainline T_1 is much longer.

spin-echo signal) as a function of t_{rep} allowed us to deduce T_1 .

For $\text{YBCO}_{6.64}:\text{Zn}$, nn resonances are seen (see Fig. 1) at low temperatures ($T < 150$ K). The relative intensity of these nn resonances could be enhanced by repeating the pulse sequence at a fast rate ($t_{\text{rep}} \sim 20$ s). Indeed, the T_1 of the outermost satellite (~ 10 s), was found smaller than that of the main line (~ 100 s). The fact that the latter has a reduced intensity in such an experimental condition thus allows us to fix accurately the position and the width of the nn resonances. The mainline being the narrowest and the most intense, its position and width were easily determined with a long repetition time, allowing full recovery of the mainline signal. Using the positions and widths of the nn resonances determined in the manner indicated above, the relative intensities of the various lines in the spectrum were determined (by fitting the lineshape to a sum of three Gaussians), for $t_{\text{rep}} > 5T_1$ of the slowest recovering component, so that all the components had fully recovered. The T_1 's of the individual lines were determined from an exponential fit of their intensities (in the FT) with respect to the repetition time. Each T_1 measurement took about 15 hours.

3 Results

In the following, we present the doping and temperature dependence of various NMR parameters in $\text{YBCO}_{6+x}:\text{Zn}$. We shall first report the existence of additional NMR lines detected in the underdoped samples. Their characteristics (shift, width, and intensity) enable us to associate them with ^{89}Y nuclei near-neighbours of the Zn substituted on

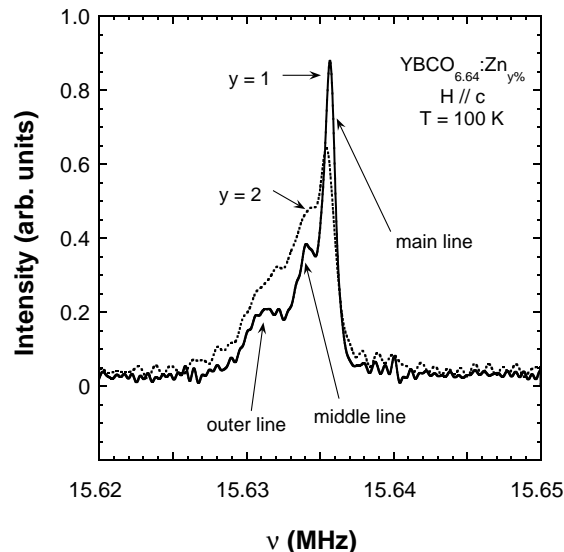


Fig. 2. ^{89}Y NMR lineshapes at 100 K in $\text{YBCO}_{6.64}:\text{Zn}_y\%$, for the sample c axis aligned parallel to the applied field H . The relative intensities of the outer and middle lines are seen to qualitatively increase with increasing y .

the CuO_2 planes (Sect. 3.1.1). The results on the main resonance line, which corresponds to ^{89}Y sites far from the substituted Zn, are reported next and compared to those in the pure system (Sect. 3.1.2). Spin-lattice relaxation data on the nn and main resonance lines are reported in Section 3.2.

3.1 Resonance line shift and width

3.1.1 Near neighbour resonances

We will argue here that the additional resonances detected in $\text{YBCO}_{6.64}:\text{Zn}$ are not seen in $\text{YBCO}_7:\text{Zn}$ and that the additional resonances are intrinsic and a direct effect of Zn substitution.

As seen in Figure 1 the nn-resonance positions depend on the sample orientation with respect to the applied field. Furthermore (see Fig. 2), the relative intensity of the outer line increases with Zn content while its position is unchanged. We also see that, $\text{YBCO}_7:\text{Zn}$ spectra (Fig. 3a) do not show additional lines in the temperature range of our measurements ($80 < T < 350$). While this is unambiguously evident for the outermost resonance, the absence of the middle resonance in spectra of $\text{YBCO}_7:\text{Zn}$ is perhaps not immediately obvious. By measuring the $\text{YBCO}_7:\text{Zn}$ lineshape with a fast repetition rate (so that the middle resonance might be enhanced, relative to the mainline, due to its shorter T_1), we see (Fig. 3b) in fact, that the lineshape of $\text{YBCO}_7:\text{Zn}$ is unaltered by fast repetition (up to one-fourth of T_1 of the mainline). If there is any change, it is in fact the high frequency tail that has a somewhat reduced relative intensity, indicating that the tail has a longer T_1 . This is in keeping with our understanding that the upper tail in the lineshape of $\text{YBCO}_7:\text{Zn}$ appears due

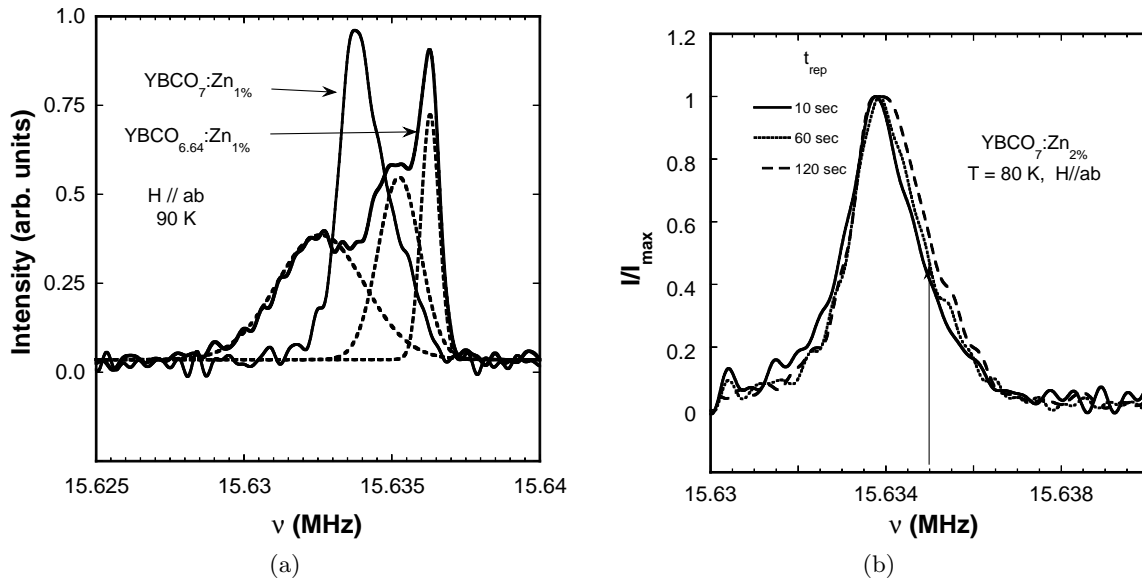


Fig. 3. (a) ^{89}Y NMR lineshape at 90 K in $\text{YBCO}_7:\text{Zn}_{1\%}$ showing absence of resolved nn lines indicating that the induced local moment magnitude is weak in $\text{YBCO}_7:\text{Zn}$ as compared to that in $\text{YBCO}_{6.64}:\text{Zn}$. Also shown is the decomposition of the lineshape for $\text{YBCO}_{6.64}:\text{Zn}_{1\%}$ into three Gaussians. (b) ^{89}Y NMR lineshape at 80 K in $\text{YBCO}_7:\text{Zn}_{2\%}$ for different repetition rates. The arrow indicates the position of the middle line in $\text{YBCO}_{6.64}:\text{Zn}$. The lineshape stays nearly unchanged indicating the absence of any components relaxing faster than the mainline.

to those regions of the sample which are not fully oxidized and hence have a longer T_1 . In short, $\text{YBCO}_{6.64}:\text{Zn}$ has additional ^{89}Y resonances while $\text{YBCO}_7:\text{Zn}$ does not. In view of the abovementioned facts, the additional resonances are not due to spurious phases since those should be present independent of the oxygen content (the deoxygenated samples are obtained merely by vacuum reduction of $\text{YBCO}_7:\text{Zn}$ at low T (< 450 °C)).

In order to identify the origin of these lines we have therefore performed quantitative analyses of the spectral intensity. Experimental lineshapes for $\text{YBCO}_{6.64}:\text{Zn}$, obtained with repetition times much longer than the spin-lattice relaxation times T_1 , were fitted to a sum of three Gaussians, where the line position and width of the two outer lines had been reliably fixed from the short repetition time spectra. The spectra along with the fits are shown in Figure 4, while the variation of their intensity as a function of Zn content is shown in Figure 5.

It is of course quite natural to expect that the most affected outer line should be associated with the Y nuclei nn to the Zn atoms. In the dilute limit, the intensity from a purely statistical occupancy of a single neighbouring site of Y by Zn, for an in plane concentration c , is $8c(1-c)^7$ for the 1st shell (curve A in Fig. 5). But, as Zn induces a significant shift of the 2nd nn Y sites as well, we also need to ensure that the 2nd nn to Y is unoccupied by Zn. The corresponding intensity for a purely random statistical occupancy would then be modified to $8c(1-c)^{15}$ (curve B in Fig. 5) which yields a smaller intensity for large Zn concentrations. We see that the intensity of the outer line is then consistent with that of the 1st nn shell, *assuming that all the Zn are substituted in the planes* (in Fig. 5

we have taken $c = 1.5y$). As for the middle resonance, the expression for the intensity due to the occupancy of a single Y 2nd nn site by Zn (with the 1st nn unoccupied) is $16c(1-c)^{23}$ in the dilute limit, which is much smaller than the experimental intensity. If the 2nd and 3rd nn are occupied by Zn with the 1st nn unoccupied, the intensity would be $(8c(1-c)^7 + 16c(1-c)^{15})(1-c)^8$ (curve C in Fig. 5). The assignment for the middle resonance is not so clear, but for dilute samples its intensity is consistent with that of total occupancy of the 2nd and 3rd nn, with the 1st nn unoccupied by Zn.

The T -dependence of the nn line-shifts shown in Figure 6 is seen to be Curie-like with a negative hyperfine coupling. This Curie-like behaviour is usually observed for local moments and justifies this denomination that we introduced in [7], although the actual magnitude and exact origin of this local moment behaviour will only become clear hereafter.

The linewidth of the nn resonances is found to increase with decreasing T (Fig. 7). The linewidth which increases with Zn concentration may be associated with the RKKY-like interaction between the Zn induced local moments. With an increase in the concentration of local moments, we might expect a frozen magnetic state (most probably a disordered spin-glass) at some point in temperature. An estimate for this is provided by a simple analysis in Section 4.5.

3.1.2 Main resonance

The temperature dependence of the shifts, $\Delta K(T)$, of the mainline for $\text{YBCO}_{6.64}:\text{Zn}$ is shown in Figure 8. As

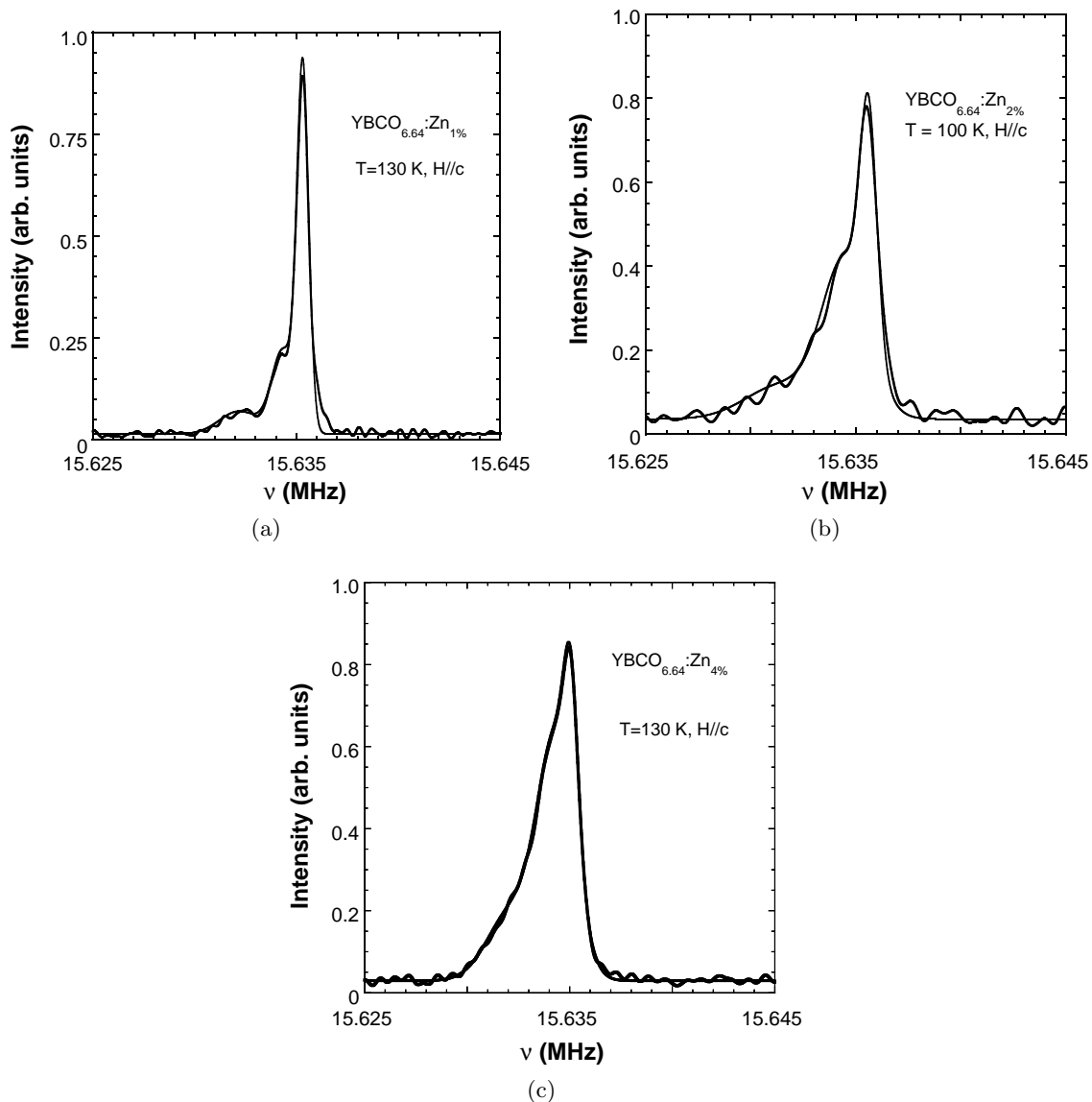


Fig. 4. Fully relaxed ^{89}Y spectra in $\text{YBCO}_{6.64}:\text{Zn}_y\%$. The solid lines are fits to three Gaussians as explained in the text. (a) 1% Zn, (b) 2% Zn, (c) 4% Zn.

reported before [7], the mainline shift does not significantly depend on the Zn content, and the average carrier density at long distance from Zn carrier density is therefore nearly unaffected by Zn substitution, at least for dilute concentrations of Zn for which the sample is still metallic. A slight offset with respect to the pure $\text{YBCO}_{6.64}$ is however evident at higher Zn doping levels and might be due to a small increase in the carrier concentration. Similar slight offsets are detected for the ^{17}O NMR shift of these compounds [27], but would rather correspond to a minute decrease in the hole content. In this latter case, a slightly incomplete oxygen loading of the starting samples might result from the fact that it has to be achieved in sealed vials, and not in a flowing oxygen atmosphere, to facilitate ^{17}O enrichment.

It should be mentioned that in reference [7], the mainline shift in an unoriented $\text{YBCO}_{6.64}:\text{Zn}_{4\%}$ sample, had

showed a slight upturn at low temperatures. Since the satellite intensities constitute a significant fraction here and cannot be clearly distinguished from the mainline, the line-position obtained from the peak did not represent the true position of the main line. In the present work, the different components of the spectra have been analysed in the fits with different repetition times so that the true position of the main resonance is deduced and shows no upturn.

The width of the mainline for $\text{YBCO}_{6.64}:\text{Zn}_y$ (see Fig. 9) has a T -dependence similar to that of pure $\text{YBCO}_{6.64}$, in that it initially decreases with decreasing temperature and then shows an increase below 120 K which is sample dependent. In the pure system, the linewidth can only be associated with a small macroscopic distribution of chain oxygen content (which we estimate of about ± 0.02 for most oxygen contents)

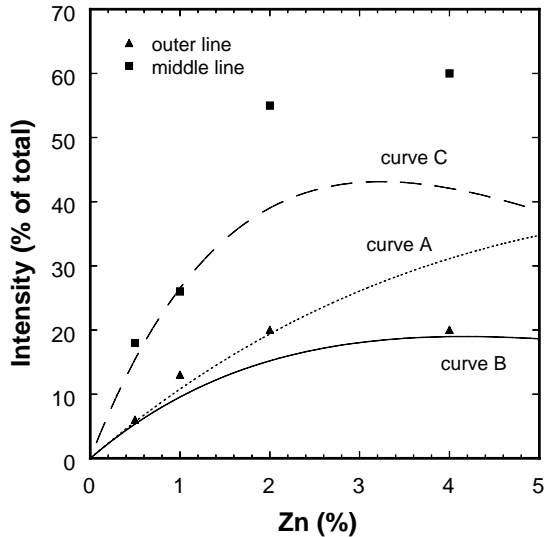


Fig. 5. Variation of the fractional nn line intensity (integrated) as a function of Zn content y for $\text{YBCO}_{6.64}:\text{Zn}_{y\%}$. The solid lines correspond to variations as expected from statistical models as explained in text. The intensity of the outermost line is seen to be in near agreement with that expected from a ^{89}Y nuclei nearest to the doped Zn. The middle line intensity might agree with that expected from a combination of 2nd and 3rd nn ^{89}Y nuclei.

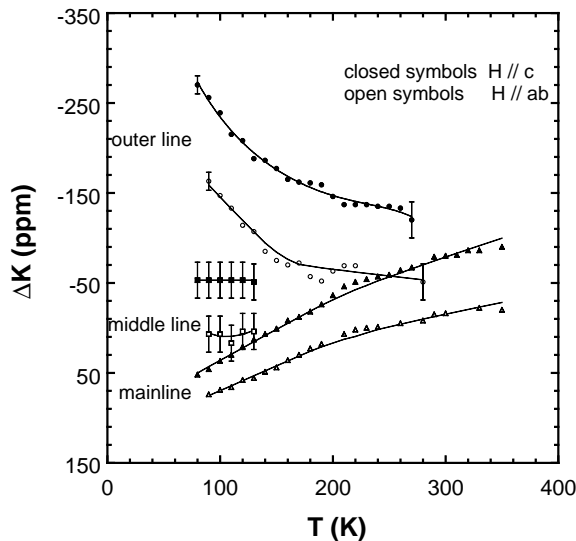


Fig. 6. ^{89}Y nn line shifts K versus temperature T for $\text{YBCO}_{6.64}:\text{Zn}_{y\%}$. The outer line shift is seen to have a strong upturn with decreasing T indicating a coupling to a Curie-like susceptibility. The solid lines are drawn as guides to the eye.

which results in a distribution of shifts at high temperatures. The T -dependencies of the shifts around the $\text{YBCO}_{6.64}$ composition are such that while the shifts are measurably different at room temperature, their magnitudes become nearly the same at low- T [1] and the NMR line becomes narrower. Therefore the width due to a distribution of oxygen content decreases at

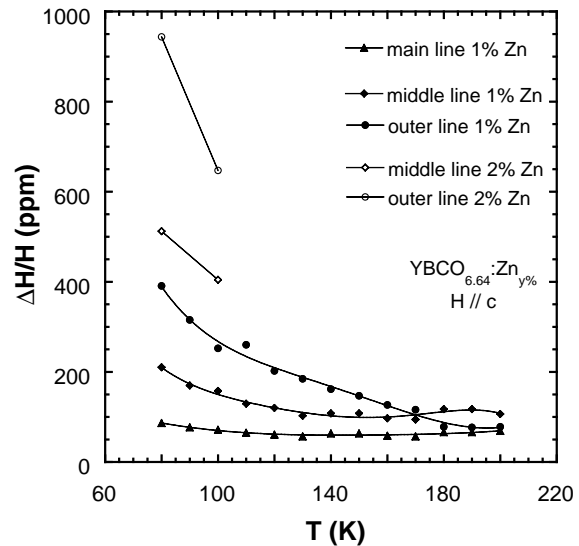


Fig. 7. Linewidths normalized to the applied magnetic field $\Delta H/H$ of the nn lines for $\text{YBCO}_{6.64}:\text{Zn}_{y\%}$ are seen to increase with decreasing T . The solid lines are drawn as guides to the eye.

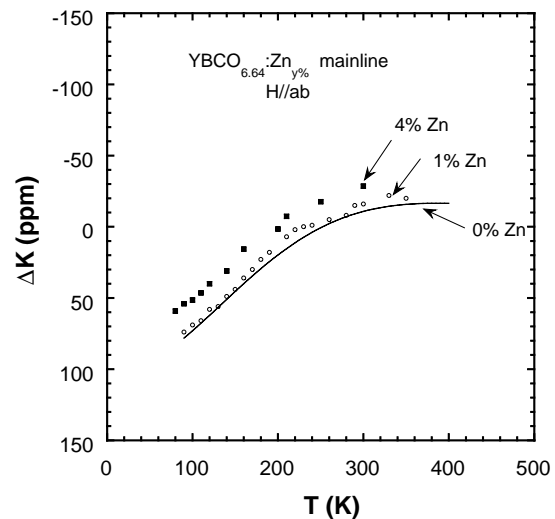


Fig. 8. ^{89}Y mainline shift K versus temperature T for $\text{YBCO}_{6.64}:\text{Zn}_{y\%}$ is nearly unchanged from that of $\text{YBCO}_{6.64}$ indicating little change in the hole content with Zn doping.

low- T . The magnitude of the width increases with Zn doping, partly due to long-distance effects of the spin-polarisation from the Zn-induced local moments. The T -dependence of the ^{17}O NMR width is found to be much larger and provides supplementary information which is analysed in detail by Bobroff *et al.* [27].

Turning to the fully oxygenated $\text{YBCO}_7:\text{Zn}$ samples, we find that here again the mainline shift is nearly independent of Zn concentration (Fig. 10). However, due to the broadening of the line at low-temperatures, we cannot unambiguously determine whether the maximum seen

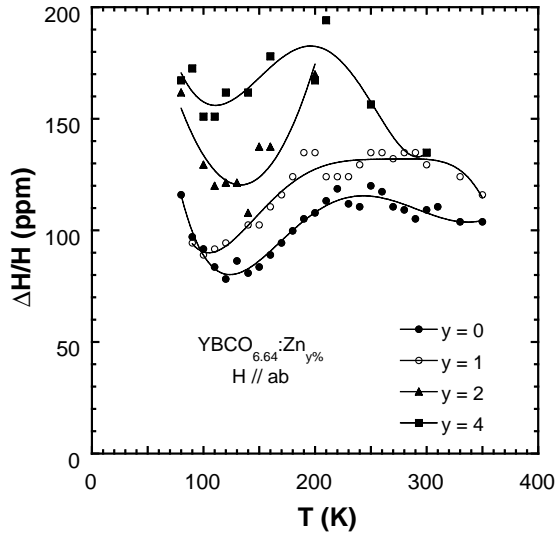


Fig. 9. Normalized linewidth $\Delta H/H$ of the mainline versus the temperature T for $\text{YBCO}_{6.64}:\text{Zn}_{y\%}$. Unlike YBCO_7 which has a nearly T independent linewidth, $\text{YBCO}_{6.64}$ linewidth decreases below 120 K and increases again at much lower temperatures. Qualitatively, the linewidths for Zn doped $\text{YBCO}_{6.64}$ are higher than the undoped compound. The solid lines are drawn as guides to the eye.

in the T dependence of ^{89}Y NMR shift of pure YBCO_7 , with $T(K_{\text{max}})$ only slightly larger than T_c (and having a possible connection to the pseudo-gap) has shifted to lower temperatures or altogether disappeared. The Curie-like broadening (Fig. 11) in $\text{YBCO}_7:\text{Zn}$ is indicative of a distribution of magnetic contributions to the line positions. This RKKY-like broadening must originate from a magnetic state which develops around the doped Zn.

For oxygen contents intermediate between O_7 and $\text{O}_{6.6}$, the T -dependence of the ^{89}Y shift in $\text{YBCO}_{6+x}:\text{Zn}$ is qualitatively similar to that in YBCO_{6+x} (Fig. 12a). However, the sharp decrease in the shift that occurs around 100 K for the slightly oxygen depleted samples ($\text{YBCO}_{6.95}$ or so) is absent in the Zn doped samples where the decrease in the shift is more gradual with T . This might again be due to the difficulty in defining accurately the oxygen content (and therefore the hole concentration) for the Zn substituted samples and especially for the large 4% Zn concentration which has been systematically investigated. As for the outer resonance, we did not perform systematic investigations *versus* oxygen content. It is however clear in the spectra of Figure 12b, that the low-frequency tail which monitors the position of this outer resonance is progressively nearer to the central line when the oxygen content is increased. Further, this outer resonance even disappears for $x = 0.92$ which corresponds to the maximum oxygen content for 4% Zn. The NMR shift of the outer resonance with respect to the mainline is therefore progressively reduced with increasing hole content.

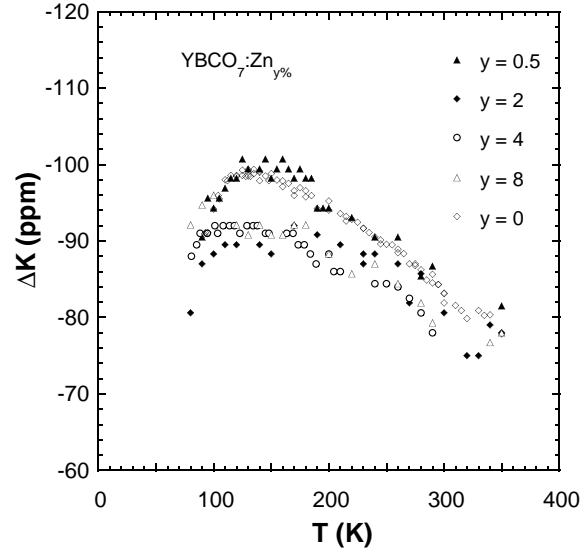


Fig. 10. The T variation of ^{89}Y mainline shift K for $\text{YBCO}_7:\text{Zn}_{y\%}$ is unchanged from that in YBCO_7 again indicating that the hole content is nearly unchanged with Zn doping. Note that the chemical shift reference is about 150 ppm, hence the change in susceptibility on Zn addition is at most 4% of the susceptibility.

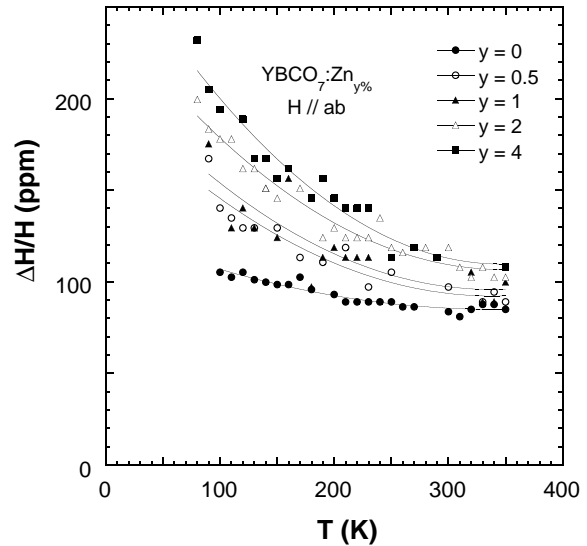


Fig. 11. Normalized linewidth $\Delta H/H$ of the mainline *versus* the temperature T for $\text{YBCO}_7:\text{Zn}_{y\%}$. The linewidth increases in a Curie-like manner with decreasing T . Also, the linewidth is larger for larger Zn contents. Solid lines are drawn as guides to the eye.

3.2 Spin-lattice relaxation

Next, we present the results of spin-lattice relaxation measurements for $\text{YBCO}_{6.64}:\text{Zn}$. The data were obtained on the nn lines and the mainline as detailed in the previous section. Representative spectra for various values of t_{rep} are shown in Figure 13. The resulting magnetisation recovery for the three lines for the data of Figure 13 are

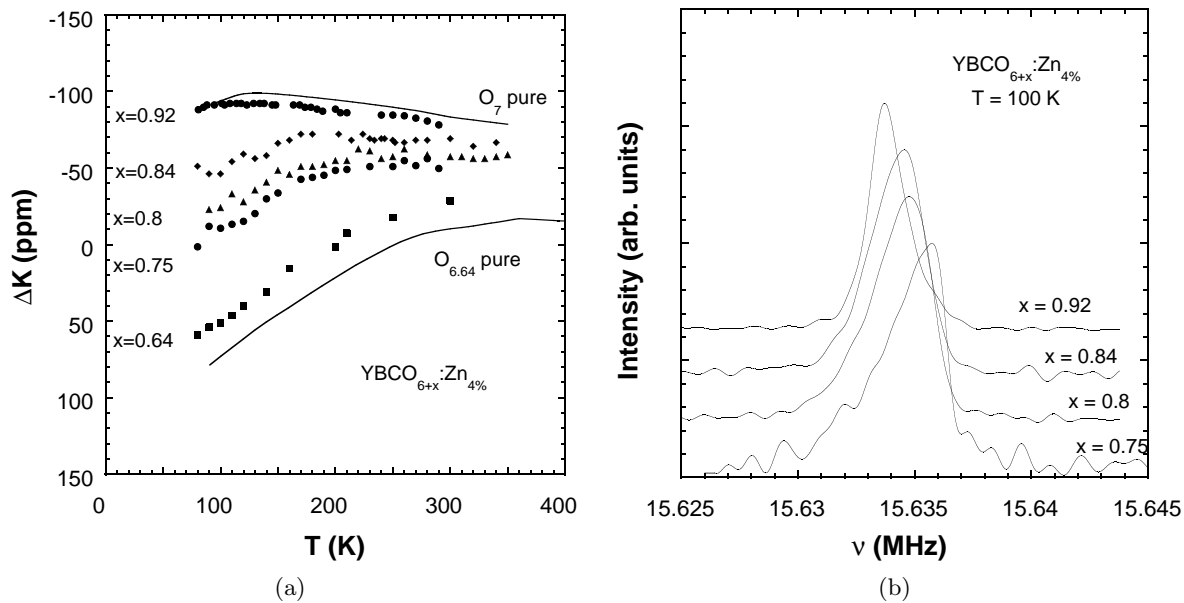


Fig. 12. (a) ^{89}Y mainline shift K versus temperature T for $\text{YBCO}_{6+x}:\text{Zn}_{4\%}$. The T -dependence is similar to that of YBCO_{6+x} . (b) Variation of lineshape as a function of x for $\text{YBCO}_{6+x}:\text{Zn}_{4\%}$. The low frequency tails which correspond to the shifted satellite lines are seen to appear already for oxygen content $x = 0.84$.

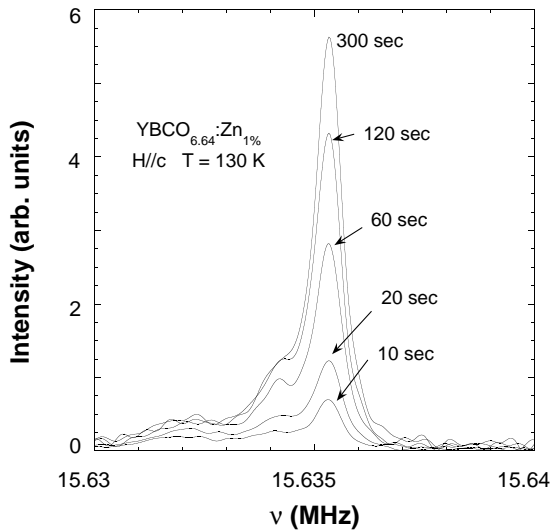


Fig. 13. Spectra for $\text{YBCO}_{6.64}:\text{Zn}_{1\%}$ for various t_{rep} values. It is clear that the outer line recovers its full intensity for much smaller t_{rep} values than the mainline and hence has a much shorter T_1 than the mainline.

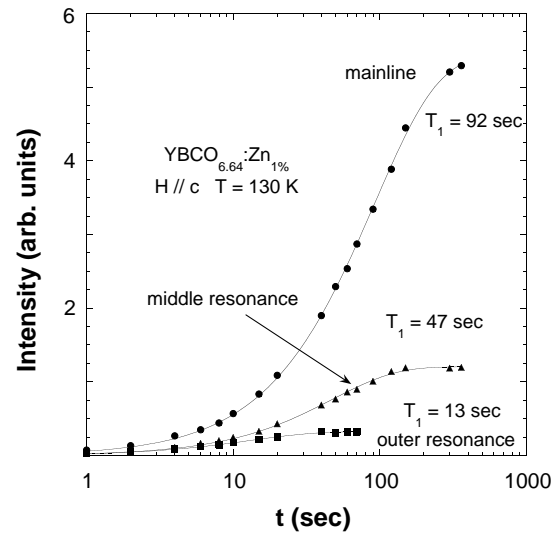


Fig. 14. Analysis of the relaxation rate data of Figure 13 for $\text{YBCO}_{6.64}:\text{Zn}_{1\%}$. The data have been fitted to a sum of three Gaussians and the deduced intensities corresponding to the main and the nn lines are plotted versus the repetition time of the pulse sequence t_{rep} on a semi-log scale. The solid lines are fits to a single exponential recovery.

shown in Figure 14. Exponential fits have been found to apply in all cases as illustrated in Figure 14.

Taking such data is obviously not straightforward. A high enough signal to noise ratio is required, as seen for our spectra displayed in Figure 13. Other publications on ^{89}Y NMR in $\text{YBa}_2\text{Cu}_4\text{O}_8:\text{Zn}$ [12,28] are completely bereft of T_1 data, which corroborates the difficulty in obtaining good data. The relaxation rate of the additional lines (other than the mainline) is seen (Fig. 15) to be strongly enhanced resulting from

local moment fluctuations as is discussed in Section 4.1.2. The outermost satellite is the most affected which indicates that it must result from having Zn as its 1st nn. The mainline T_1 is nearly unaffected which shows that, for dilute concentrations of Zn, the planar dynamic susceptibility far from Zn is unaffected, in accordance with the NMR shift data.

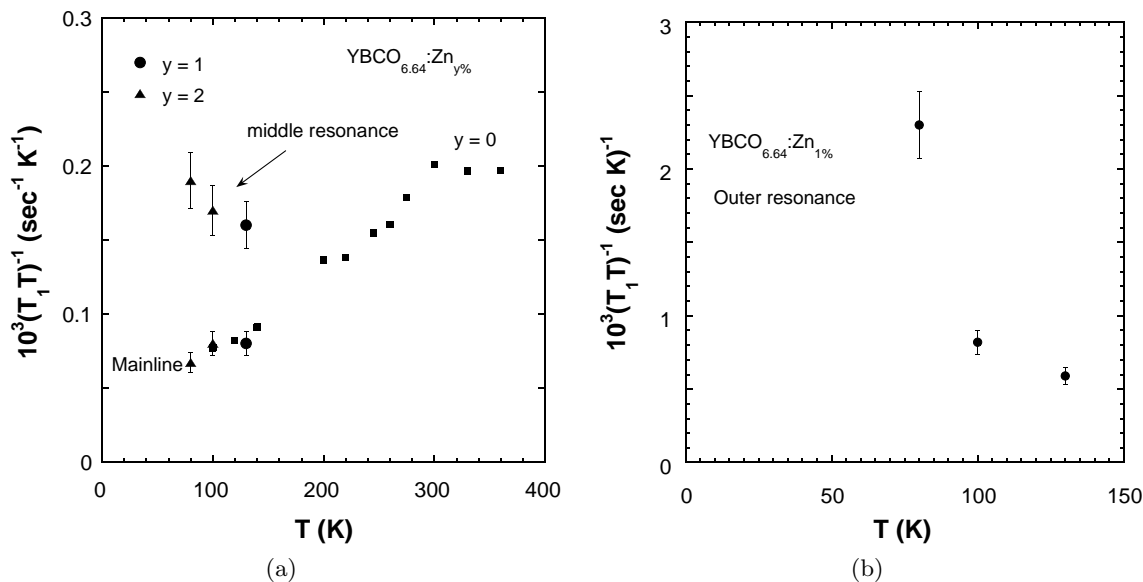


Fig. 15. (a) ^{89}Y nuclear spin-lattice relaxation rate divided by temperature $1/T_1T$ versus temperature T for the mainline and the middle satellite in $\text{YBCO}_{6.64}:\text{Zn}_{y\%}$. (b) these data are for the outermost satellite line. The nn lines are seen to have a shorter T_1 than the mainline.

In YBCO_7 , Dupree *et al.* [10] measured the effect of Zn doping on T_1 at room temperature. They found that the ^{89}Y spin-lattice relaxation rate was strongly enhanced on Zn substitution. However, our data were in complete disagreement with theirs. We therefore repeated measurements on various batches of samples and at various temperatures. In all cases we found that the nuclear magnetisation recovery fits well to a single exponential (Fig. 16) and that the resulting T_1 and its T -dependence is not significantly different from that of pure YBCO_7 , as can be seen in Figure 17. We must therefore conclude that limited accuracy was responsible for the observation done by Dupree *et al.* [10]. As there are no discernible resonances in addition to the main line in these experiments on $\text{YBCO}_7:\text{Zn}$, the implication is a much weaker induced moment in YBCO_7 , compared to $\text{YBCO}_{6.64}:\text{Zn}$, in agreement with our bulk susceptibility data [9,16].

4 Analysis of the experimental results

4.1 Local moments in $\text{YBCO}_{6.64}:\text{Zn}$

4.1.1 nn NMR shifts

We recall here, that the distinct, well defined resonances that we have observed in $\text{YBCO}_{6.64}$ correspond to Y near neighbour sites of the substituted Zn. The Curie-like T -dependence of the position of the first near-neighbour line, and the shortening of its T_1 at low- T are striking experimental evidence of the occurrence of Zn induced local moments. The location, spatial extent and dynamics of these moments in $\text{YBCO}_{6.64}$ will be discussed first. Occurrence of local moments for the slightly overdoped composi-

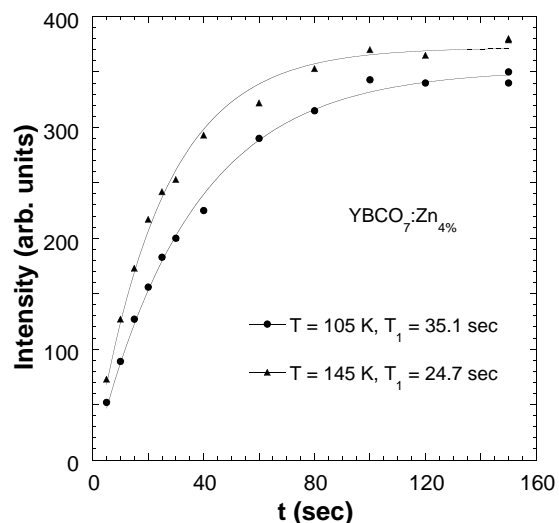


Fig. 16. Nuclear magnetization corresponding to the mainline versus the repetition time of the pulse sequence t_{rep} for $\text{YBCO}_7:\text{Zn}_{y\%}$. The fact that the data can be fit to a single exponential (solid line) indicates the absence of any other components to the relaxation.

tion YBCO_7 is also established through the induced long-distance perturbation of the host-spin-magnetization.

The Zn induced local moments are quite clearly located in the vicinity of the Zn, and dominantly on the four nearest neighbour O or Cu orbitals. In what follows, we shall perform extensive comparisons of the ^{89}Y NMR shift with the Zn induced Curie contribution to the spin

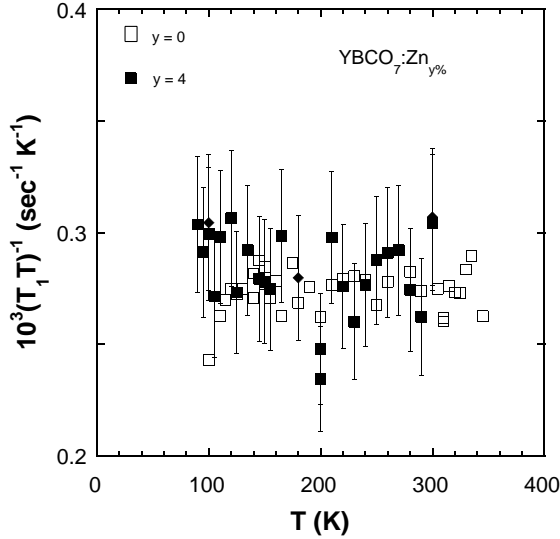


Fig. 17. ^{89}Y nuclear spin-lattice relaxation rate divided by temperature $1/T_1 T$ versus temperature T for $\text{YBCO}_7:\text{Zn}_{y\%}$. Note the magnified scale of the y axis. As for $\text{YBCO}_{6.64}:\text{Zn}$, the T_1 of the mainline is not affected.

susceptibility (expressed per mole Zn) [9,16],

$$\chi_c = \frac{C_M}{T} = \frac{N_A p_{\text{eff}}^2}{3k_B T}. \quad (1)$$

Here N_A is the Avogadro number and p_{eff} is the effective moment. These comparisons will allow us first to rule out a localisation of the moments on the O orbitals and then to demonstrate that the local moment is distributed on the Cu orbitals. Furthermore, assuming that the transferred hyperfine couplings are not modified by Zn substitution, we will show that our analysis is consistent with a locally AF state extended over a few lattice sites.

A local moment could also be present around Zn if a hole were trapped on the near-neighbour oxygen orbitals. Two quite different physical situations would occur, depending on whether the local moment is located on the p_π or p_σ orbitals. Since the p_π are directly admixed with the Y s orbitals, a strong positive hyperfine coupling would result, contrary to our observation of a negative Curie contribution to the shift. Therefore, the present experiment implies that this shift component can only be induced through the oxygen p_σ orbitals.

In undoped YBCO_{6+x} , the Y NMR shift arises from a coupling of the Y nuclear spin with the small fraction of holes on the $\text{O}(2p_\sigma)$ orbitals due to their *covalency* with the $\text{Cu}(3d_{x^2-y^2})$ holes, while the spin-polarization of the doped holes themselves is negligible [1]. This has been deduced from the fact that the covalent admixture of the $\text{O}(2p_\sigma)$ orbital with the $\text{Cu}(3d_{x^2-y^2})$ orbital is about 10% [29], which implies that the hyperfine coupling to the oxygen holes should be 10 times larger than its coupling to the $\text{Cu}(3d_{x^2-y^2})$ holes.

Let us first consider the possibility that the Curie contribution comes from holes localised on the four $\text{O}(2p_\sigma)$ orbitals near Zn. The 1st nn Y site has six O nn which we

assume are nearly unaffected by Zn and two O nn which would exhibit Zn induced Curie magnetism. The net ^{89}Y shift would be written as

$$\Delta K_1^\alpha = (6/8)K_s^\alpha + K_c^\alpha + \delta_1^\alpha \quad (2)$$

where index α refers to a principal direction, K_s^α is the spin shift of the mainline, $K_c^\alpha = 2C_s^\alpha/T$ is the Curie contribution to the spin shift due to its two 1st nn O with a moment, and δ_1^α is the chemical shift. A least-squares fit to the data in Figure 18a allows us to extract the two unknown parameters C_s^α and δ_1^α . The chemical shift values thus obtained are δ_1^c (δ_1^{ab}) = 144 (163) \pm 10 ppm. The values of C_s^α are found to be -14000 (-12300) \pm 500 ppm K for $H \parallel c$ ($H \parallel ab$).

Let us compare then these shifts with the macroscopic susceptibility χ_c , with $\mu_B K_c = 2H_{\text{hf}}\chi_c/4$, if the moment is distributed on the four $\text{O}(2p_\sigma)$ near neighbour orbitals to the Zn. Using $C_M = 9.2 \times 10^{-2}$ emu K/mole Zn [9,16] and the Curie term in the shift deduced above, we get $H_{\text{hf}} = -1.6$ kG. This is of the order of the hyperfine coupling expected with Cu and nearly 10 times smaller than that expected with oxygen. Moreover, we point out that a 2nd nn Y to Zn would not be coupled to the moment on the oxygen (a local moment on oxygen is unlikely to be spread over more than 4 sites since it would presumably arise from hole localisation). Hence, a second line in addition to the main line should not be observed, contrary to the data from our experiment. One could imagine that one has both, localised hole and weakly affected nn Cu. But this would require a large susceptibility on the Cu to give the strong shift of the 2nd nn line compared to the mainline. This eliminates the oxygen p_σ as a possible site for local moments.

If, however, the satellite shift is modelled as coming from a hyperfine coupling to the local moments residing on the Cu $d_{x^2-y^2}$ orbitals, the relevant equation for the 1st nn shift in our model is

$$\Delta K_1^\alpha = (5/8)K_s^\alpha + K_c^\alpha + \delta_1^\alpha. \quad (3)$$

From a fit of the data to this equation, the chemical shift values obtained (see Fig. 18b), δ_1^c (δ_1^{ab}) = 100 (140) \pm 10 ppm, are only slightly different from δ_1^c (δ_1^{ab}) = 165 (150) ppm found in the pure material [7]. The values of C_s^α are found to be -13100 (-11600) \pm 500 ppm. This implies a hyperfine field $H_{\text{hf}} \approx -3.2$ kG/Cu which is slightly larger than that for the pure material (≈ -2 kG). Such a modification of H_{hf} could be attributed to a corresponding change of the $\text{Cu}(3d_{x^2-y^2})$ - $\text{O}(2p_\sigma)$ hybridisation due to a displacement of the 1st nn oxygen to Zn. Alternatively, if the hyperfine coupling stays unchanged, the actual susceptibility on the 1st nn Cu, $\chi(1)$, is larger than $\chi_c/4$. This would imply that further copper ions would have a magnetization anti-parallel to the applied field, which might be expected if the local moment develops as an AF correlated cloud of copper lattice sites. Considering this possibility, the Cu 2nd nn to Zn will bear a small negative susceptibility $\chi(2)$.

Figure 19 illustrates schematically the location and the orientation of the Zn induced local moments. In such a

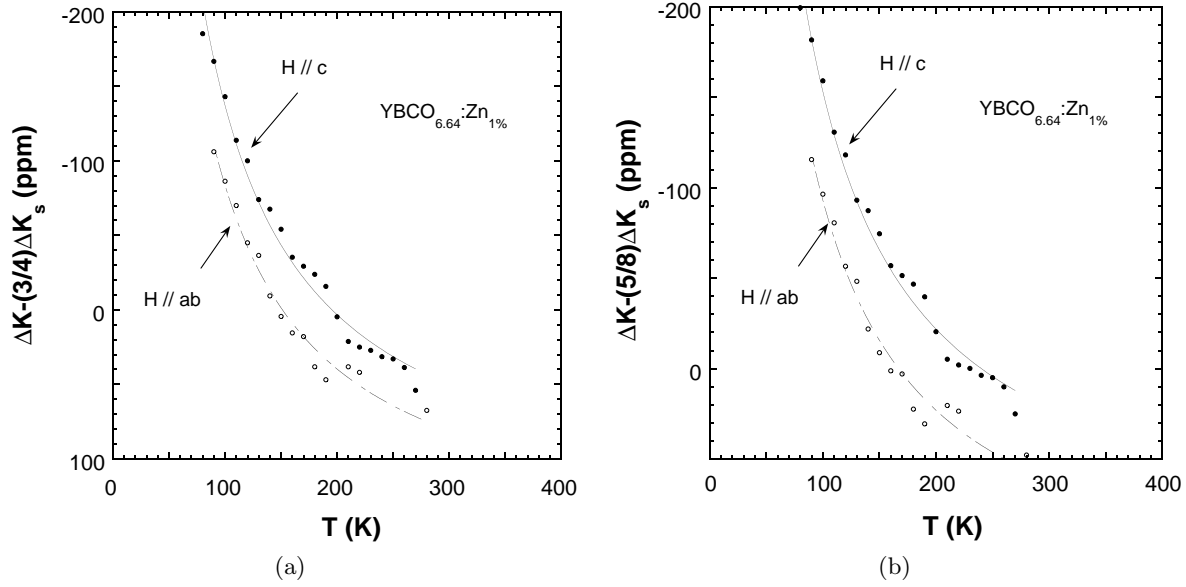


Fig. 18. (a) Curie component (in addition to a constant) of the ^{89}Y shift K versus temperature T for the outermost line in $\text{YBCO}_{6.64}:\text{Zn}_{1\%}$. The solid line is a fit (see Eq. (2)) assuming that the local moment is on the oxygen atoms. (b) The solid line is a fit (see Eq. (3)) assuming moments on the copper atoms.

model, the shifts of the 1st and the 2nd nn Y will be as follows:

$$\Delta K_1^\alpha = (4/8)K_s^\alpha + 2K_1^\alpha + K_2^\alpha + \delta_1^\alpha \quad (4)$$

$$\Delta K_2^\alpha = (6/8)K_s^\alpha + K_1^\alpha + K_2^\alpha + \delta_2^\alpha. \quad (5)$$

Here we can differentiate the hyperfine fields for the first and second nn using $\mu_B K_1^\alpha = H_{\text{hf}}(1)\chi(1)$ and $\mu_B K_2^\alpha = H_{\text{hf}}(2)\chi(2)$. We can then fit $\Delta K_1^\alpha - (4/8)K_s^\alpha$ to a Curie term in addition to a constant and likewise for $\Delta K_2^\alpha - (6/8)K_s^\alpha$. A fit of the observed shifts of the 1st and the 2nd nn Y to these equations yields the following values for the corresponding Curie terms; $C_1^c = -14,530$ ppm K, $C_2^c = +4630$ ppm K. The corresponding chemical shifts for the 1st and the 2nd nn Y are found to be 75 and 144 ppm, respectively. Assuming the same hyperfine coupling for 1st nn and 2nd nn Y, $\chi(2) = -\chi(1)/3$ and therefore the macroscopic susceptibility $\chi_c = 8\chi(1)/3$. Using $\mu_B K_1^\alpha = H_{\text{hf}}(1)\chi(1)$, we get a hyperfine field of about -2.35 kG which is closer to the value of -2 kG in the undoped compound. Although this picture is then compatible with the experimental results, the accuracy of the data is not sufficient to ascertain its validity. The fact that the intensity of the middle resonance cannot be assigned solely to the 2nd nn of Zn implies that further near neighbour sites of the Zn should be taken into account. More accuracy would also be required to take into account the 3rd nn and try to estimate the size of the AF correlated region around the Zn site.

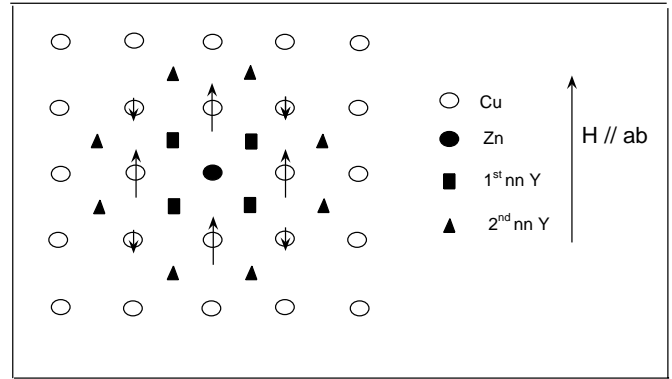


Fig. 19. A schematic of the location and the orientation of the local magnetization around a Zn impurity.

4.1.2 Spin-lattice relaxation

We next turn to a discussion of the spin-lattice relaxation rate which is expressed as,

$$\frac{1}{T_1 T} \propto \sum_{\mathbf{q}} A^2(\mathbf{q}) \frac{\chi''(\mathbf{q}, \omega)}{\omega} \quad (6)$$

where $A(\mathbf{q})$ is the coupling to the magnetic fluctuations at wave vector \mathbf{q} [30]. The O and Y nuclei are at symmetry positions with respect to Cu so that $A(\mathbf{q}_{\text{AF}}) = 0$, and the fluctuations at \mathbf{q}_{AF} are filtered at these two sites. Consequently, in YBCO_{6+x} , the T -dependence of $(T_1 T)^{-1}$ for Y and O is different from that of Cu which is dominated by the fluctuations at \mathbf{q}_{AF} [5]. On adding Zn, the symmetry around the 1st nn Y is broken and this Y site becomes then sensitive to the magnetic fluctuations on the neighbouring copper ions (either intrinsic to the pure compound

or due to the local moment). Similarly, the magnetic fluctuations are no longer symmetric on the 2nd nn, so that the enhanced relaxation rate at this site is also connected to local moment fluctuations.

The sharp increase of $(T_1 T)^{-1}$ at low- T on the Y nn nuclei (much faster than the corresponding variation on the ^{63}Cu nuclei in the pure compounds) is a direct proof that the local moment fluctuations are *not* those of the Cu hole spins of the pure compound. The very existence of a Curie contribution to the spin susceptibility indeed clearly points out that the fluctuation of the Cu hole spins in the vicinity of the Zn are much slower than those of the pure host. The present data for $(T_1 T)^{-1}$ on the near-neighbour nuclei are then good proof of the slow fluctuations of the local moment.

In the case of local moments in noble metal hosts, the spin-lattice relaxation of host nuclei nearby the local moment is totally dominated at low- T by the fluctuations of the local moment (the usual Korringa process *via* conduction electrons is somewhat smaller) [38]. The situation here is quite similar for the Y 1st nn of the Zn. We can therefore consider that this nuclear spin is coupled to the 2 nn coppers which bear susceptibilities $\chi_c(\mathbf{q}, \omega)$ if we neglect the contribution to T_1 of the uncompensated Cu spin 2nd nn to Zn (Fig. 19). The relaxation rate at low- T is then given by,

$$\frac{1}{T_1} = \frac{2k_B T}{\hbar^2} \left(\frac{\gamma_n}{\gamma_e} \right)^2 H_{\text{hf}}(1)^2 \Sigma \left(\frac{\chi_c''(\mathbf{q}, \omega)}{\omega} \right) \quad (7)$$

where γ_n/γ_e is the ratio of the nuclear and the electronic gyromagnetic ratios and $H_{\text{hf}}(1)$ is the hyperfine coupling. In the limit $\omega \rightarrow 0$, the summation is given by $\chi_c(T)\tau/2\pi$ where $\chi_c(T)$ is the local moment susceptibility and τ is the relaxation time of the local moment spin. The fluctuation rate of the local moment spin is usually made up of two contributions

$$\frac{1}{\tau} = \frac{1}{\tau_{\text{ex}}} + \frac{1}{\tau_{\text{int}}} \quad (8)$$

where the first term corresponds to the single Zn impurity local moment relaxation to the host spin bath, for instance through the exchange with the conduction electron spins and the second would correspond to fluctuations due the coupling between the Zn induced local moments which depends on Zn concentration.

For instance, for dilute local moments in noble metal hosts

$$\frac{1}{\tau_{\text{ex}}} = \left(\frac{4\pi}{\hbar} \right) (k_B T) (J_{\text{ex}} \rho(\epsilon_F))^2 \quad (9)$$

if a Korringa relation holds (J_{ex} is the coupling of the local moments to the band). In that case, the second term is $\tau_{\text{int}}^{-1} = \omega_{\text{int}}/2\pi$ with $\omega_{\text{int}}^2 = 8J_{\text{int}}^2 z S(S+1)/3\hbar^2$ where $z \propto c$ is the number of nearest neighbour spins and J_{int} is the conduction electron mediated coupling between impurity spins.

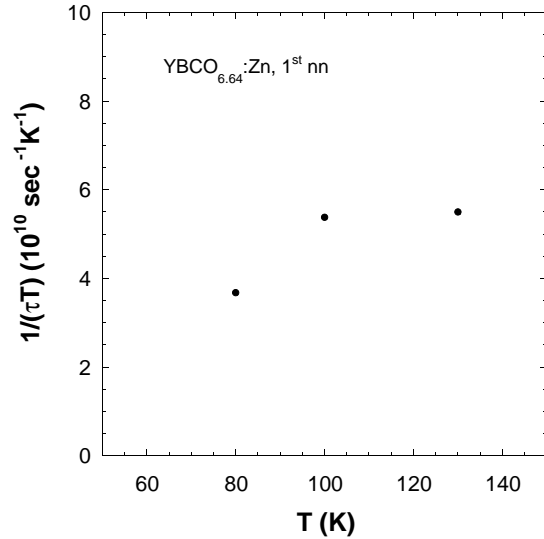


Fig. 20. The ratio of the relaxation rate of the local moment spin $1/\tau$ to temperature T for the 1st nn ^{89}Y nuclei in $\text{YBCO}_{6.64}:\text{Zn}$. τ has been determined from equation (10).

In our case, the T_1 values for the near neighbour resonances did not depend markedly on the Zn content, so that the single impurity induced relaxation $1/\tau_{\text{ex}}$ dominates the results. Further, the local moment spin susceptibility is Curie-like down to low temperatures. A small Curie-Weiss correction $\chi = C/(T + \theta)$ with $\theta \simeq 4$ K is observed for $\text{YBCO}_{6.64}:\text{Zn}_{4\%}$ [9]. This is in agreement with the observed spin freezing temperature of about 3 K in the sample [9]. All these results therefore allow to conclude consistently that the spin-lattice relaxation is dominated by the spin fluctuations of the isolated Zn induced local moment. This should then be written as

$$\frac{1}{T_1} = \frac{2k_B T}{\hbar^2} \left(\frac{\gamma_n}{\gamma_e} \right)^2 H_{\text{hf}}(1)^2 \frac{\chi_c(T)\tau_{\text{ex}}}{2\pi}. \quad (10)$$

Since $\chi_c T$ is constant, $1/T_1$ is proportional to τ_{ex} . In the conventional metallic case, where $\rho(\epsilon_F)$ is independent of the temperature, the spin-lattice relaxation rate $1/T_1$ of the host nuclei (near impurities) is observed to follow a Curie-like law $1/T_1 \propto C/T$ [38]. The present case is clearly more complicated since the host metal itself is strongly correlated, which results in the pseudo-gap of the static spin susceptibility and in the $1/(T_1 T)$ behaviour for the ^{63}Cu . As the local moment positions are commensurate with the Cu hole spin system, we might anticipate that a similar anomaly might occur for $1/(\tau_{\text{ex}} T)$, which scales with T_1/T . We have therefore plotted in Figure 20 this quantity for the three data points for Y near neighbours to Zn. Although the data are clearly insufficient, they suggest a maximum for $1/(\tau_{\text{ex}} T)$, quite analogous to that seen for ^{63}Cu T_1 .

4.2 Comparison with other experiments

Following our early report [8], some related experiments have been performed on the impurity substituted

cuprates. In various cases, the authors have drawn conclusions which are not in complete agreement with our results and sometimes disagree totally. These contradictions are therefore considered in the following.

4.2.1 Gd ESR

Janossy *et al.* [14] have done Gd^{3+} ESR, in 1% Gd substituted YBCO_{6+x} , which are in principle quite similar to our experiments. Indeed, the Gd electronic moment and the ^{89}Y nuclear spin are coupled to the copper hole spins by similar transferred couplings. They find that the g -shift of the Gd ESR has the same T -dependence as the ^{89}Y NMR shift. They have therefore used the Gd probe in $\text{Y}_{0.99}\text{Gd}_{0.01}\text{BaCuO}_{6+x}:\text{Zn}$ samples as well. The Gd spectrum should result from a simple scaling with the ^{89}Y NMR spectrum through the ratio of the hyperfine couplings, as the relative positions of the main and satellite lines scale as the ratio of (νH_{hf}) where ν is the operating frequency and

$$(\delta\nu/\nu) = H_{\text{hf}}\chi. \quad (11)$$

The fact that they did not detect any nn resonances might cast some doubt on the meaning of our results. However, we insist here that one should also consider scaling of the relaxation rates to arrive at reliable conclusions. The relaxation rates scale as

$$1/T_1 \propto (\gamma H_{\text{hf}})^2 \quad (12)$$

and therefore contribute quite differently to the broadening of the spectra. In the case of NMR, the linewidth $\Delta\nu$ is governed by the susceptibility distribution which scales as $\delta\nu$, while in ESR, the T_1 process is so efficient that it contributes significantly to (and even dominates) the ESR linewidth. Using our detailed data for ^{89}Y nn NMR, we can easily calculate the expected contributions for the Gd nn ESR, through equations (11, 12). Here we shall use [14], $^{\text{Gd}}H_{\text{hf}} = 10^{\text{Y}}H_{\text{hf}}$ and $\gamma_e = 1.6 \times 10^4 \gamma$. Using the operating frequencies, $\nu = 15.64$ MHz for ^{89}Y NMR and $\nu = 245$ GHz for Gd ESR, we can deduce the satellite separation from the main line and the static and T_1 contributions to the linewidth at 100 K. These are reported in Table 1. We find then that the expected width for the Gd ESR nn line is at least four times larger than its shift, which justifies that the satellite resonances are indeed quite difficult if not impossible to observe.

The other issue is the suggestion by Janossy *et al.* that the susceptibility corresponding to the pure YBCO_7 is restored at the Cu neighbouring Zn. Since we observe a Curie-like increase of the nn line shift in Zn doped samples, increasing to values well above the YBCO_7 shift, the implication is that the hole content near the Zn dopants has not been restored to that of undoped YBCO_7 .

4.2.2 NMR in Al doped $\text{La}_{2-x}\text{Sr}_x\text{CuO}_4$

Recently, Ishida *et al.* [13] have performed NMR experiments on $\text{La}_{2-x}\text{Sr}_x\text{CuO}_4$ (LASCO), in which non-magnetic Al is substituted on the Cu site of the CuO_2

Table 1. ^{89}Y NMR measured values (at about 100 K) of the separation of the 1st nn line from the mainline $\delta\nu$, the spin-lattice relaxation rate of the 1st nn $1/T_1$, and the linewidth of the 1st nn $\Delta\nu$ are listed along with calculated values (see text) of the same for Gd ESR in $\text{YBCO}_{6.64}:\text{Zn}$.

Parameter	$\delta\nu$ (Hz)	$1/T_1$ (Hz)	$\Delta\nu$ (Hz)
^{89}Y NMR	4×10^3	0.1	2×10^3
Gd^{3+} ESR	6.4×10^8	2.56×10^9	2.56×10^9

planes. Although they were unable to detect the nn nuclei of Al, they could directly detect the ^{27}Al NMR signal. They did find that the shift of the ^{27}Al NMR has a Curie component. Since Al itself does not bear a local moment, this observation can only result from a local moment which resides either on the nn oxygen or copper orbitals which are coupled to the ^{27}Al nuclear spin *via* transferred hyperfine couplings. This observation does not enable one to decide the location of the local moment. However, by analogy with our results, the authors have inferred that it is located on the nn Cu orbitals. Their data are important as they confirm that a non-magnetic substituent induces a local moment in a cuprate different from YBCO_{6+x} . Ishida *et al.* [13] measured the ^{27}Al NMR shift and T_1 which can be compared with the corresponding data on the nn ^{89}Y NMR in YBCO_{6+x} . As we stress below, several qualitative differences in the experimental results are evident.

First, they analysed the T -dependence of the shift and susceptibility in Al doped LASCO with a Curie-Weiss law with a sizeable Weiss temperature ($\theta \approx 50$ K). It is not so clear whether this high value of θ is also suggested by the ^{27}Al NMR results since it might be influenced by the reference taken for the ^{27}Al chemical shift. In any case, Ishida *et al.* do not demonstrate whether this large θ corresponds to a genuine single impurity effect or if it varies with Al content thereby revealing a large coupling between the local moments. In underdoped YBCO, we never found any indication for such a large deviation from the Curie law, neither from NMR nor from susceptibility data. A negative value $\theta \approx -30$ K has been found by Monod *et al.* [31] in $\text{YBCO}:\text{Zn}$ by susceptibility measurements. However recent data on samples with low content of impurity phases, by Mendels *et al.* [9], establish that a significant estimate of θ requires a correct accounting of the susceptibility contribution of the pure compound. They deduced $\theta \simeq 4$ K for $\text{YBCO}_{6.64}:\text{Zn}_4\%$.

In order to analyse the ^{27}Al relaxation rate data, Ishida *et al.* use the simple local moment formulation of Equations (7-10) (with different notations). They provided a quantitative analysis of their data in which the value of J_{int} as deduced from their value of τ_{int} (a microscopic probe) is fully consistent with their value of θ (from bulk susceptibility, a macroscopic probe). This analysis would then appear to be consistent with and support a simple local moment picture. We stress here that not only do their results differ *qualitatively* from ours but that an alternative interpretation is possible [32]. In their analysis, they

deduce a relaxation rate $1/\tau$ which only varies slightly with T . This would be expected if it were dominated by the τ_{int} term which is expected to be T -independent in the classical local moment picture. Our results, on the other hand, have exhibited a totally opposite trend with the τ_{ex} being negligible. We further find that in their T_1 analysis, Ishida *et al.* have taken a local moment Curie susceptibility while their own ^{27}Al data yielded a large Curie-Weiss temperature ($\theta = 50$ K). Introducing the actual $1/(T+50)$ dependence of χ in equations (7-10) lead us to deduce $1/(\tau_{\text{ex}}T) = 2 \times 10^{10} (\text{s K})^{-1}$ which corresponds to a T dependent contribution to $1/\tau$ which is one order of magnitude larger than their own result. This would yield a rather large value $J_{\text{ex}} = 0.17$ eV which contradicts their expectations.

However, such an analysis yields only a modest modification of the T -independent contribution which becomes $1/\tau_{\text{int}} = 5.6 \times 10^{12} \text{ s}^{-1}$, only a factor of two smaller than their result which still corresponds to a sizeable value of θ , the Weiss temperature. Of course, a significant difference between the two systems ($\text{YBCO}_{6.64}$ and LASCO) is their doping range. While $\text{La}_{1.85}\text{Sr}_{0.15}\text{CuO}_4$ should be considered close to an optimally doped material, in $\text{YBCO}_{6.64}$ we are clearly in the underdoped regime which usually displays qualitatively different properties. Unfortunately we do not have as complete results on $\text{YBCO}_7:\text{Zn}$, which would allow for a direct comparison between the two systems.

4.3 The case of $\text{YBCO}_7:\text{Zn}$

We have then clearly demonstrated that local moments are induced on Zn substitution in $\text{YBCO}_{6.64}$. We have not studied samples with oxygen contents other than 6.64 and 7 in great detail. However, we have seen, from measurements on unoriented samples (see Fig. 12b), that the low-frequency tail of the spectra which is associated with the outer satellite resonance is less shifted from the main resonance position for increasing oxygen content. We can then conclude that the local moment value decreases gradually with increasing x . On reaching YBCO_7 , we find that the nn lines have practically merged with the main line. This is confirmed from magnetisation data on impurity-phase free samples by Mendels *et al.* [9,16], which show that the Curie constant for $\text{YBCO}_7:\text{Zn}$ is about one-sixth that of $\text{YBCO}_{6.64}:\text{Zn}$. Assuming the same hyperfine couplings, the expected first nn line position is shown in Figure 21. In view of the width due to a distribution of oxygen content, it is evident that it will be difficult to resolve any extra resonance even for lower Zn contents. Going to lower temperatures is ruled out as well due to the relatively high T_c of the samples.

We did not succeed either in distinguishing the nn resonance from a contrast of relaxation rate with the mainline. We shall see here that such a contrast is not expected if we estimate the relaxation rate for the outermost resonance by scaling the $\text{YBCO}_{6.64}:\text{Zn}$ data at 100 K. The Curie term in $\text{YBCO}_7:\text{Zn}$ is about one-sixth that in $\text{YBCO}_{6.64}:\text{Zn}$ and the density of states at the Fermi level

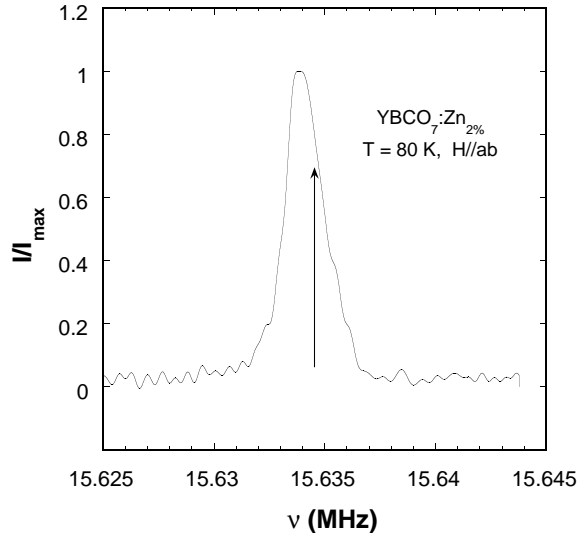


Fig. 21. ^{89}Y NMR spectrum for $\text{YBCO}_7:\text{Zn}_{2\%}$. Expected position of outermost line, based on the macroscopic susceptibility data (see text) is indicated by an arrow. The actual linewidth even in the pure compound is such that any feature at this position cannot be resolved.

$\rho(\epsilon_F)$ can be estimated about 3 times higher, from the ^{89}Y NMR shift data. Assuming that the local moment to band coupling J_{ex} stays unchanged, Equations (9, 10) allow to deduce a contribution of the local moment fluctuations to $1/T_1$ of $\approx 0.0018 \text{ s}^{-1}$, which is much smaller than the observed rate in undoped YBCO_7 (0.03 s^{-1}). This confirms that for $\text{YBCO}_7:\text{Zn}$, local moment fluctuations are indeed difficult to detect on the nn Y site.

In fact, the occurrence of a local moment in $\text{YBCO}_7:\text{Zn}$ was evidenced first [7] from the presence of the oscillating long distance RKKY spin polarisation of the host Cu spins. This was established from the Curie like increase of the ^{89}Y NMR linewidth observed in $\text{YBCO}_7:\text{Zn}$, and is confirmed in the present experiments as well as from ^{17}O NMR linewidth [33] data.

4.4 About AF correlations near the Zn impurities

The experimental results on Gd ESR in YBCO and Al NMR in Al doped LASCO have been interpreted along quite different lines. For Janossy *et al.*, the absence of a Curie term for the ESR line shift led them to conclude that there was no local moment. Instead, they considered that the susceptibility of the YBCO system is restored near the Zn, as they found an increase of the ESR shift with decreasing T . On purely experimental grounds it is not clear whether the detected ESR signal involves all the Gd spins. We have seen above that the outermost nn resonances are not expected to be resolved in the ESR data. However, the inner resonance might contribute to a wing in the signal, and might explain the observed shift.

In any case, the present detailed ^{89}Y NMR data demonstrate that the central line is not shifted at all, so that the susceptibility is unmodified at a few lattice

distances from the Zn impurity. Second, the Curie-like increase of the shift for the nn reaches values well above those observed for pure YBCO_7 , which implies that the hole content near the Zn dopants has not been restored to that of undoped YBCO_7 . Finally, the bulk susceptibility data (measured using a commercial SQUID magnetometer) of Mendels *et al.* [9] indicate that the local moment susceptibility increases down to 10 K, so that there is no doubt about the occurrence of a Curie contribution. The fact that the nn lines broaden strongly with decreasing temperature is sufficient to explain that the Gd ESR picks up only a part of the Gd signal which saturates at low- T . This is somewhat reminiscent of the situation which prevailed in the preliminary ^{89}Y NMR measurements done for large Zn concentrations in YBCO [7]. In that case, the nn resonances were not resolved and an apparent shift of the ^{89}Y NMR signal was observed. As the broadening of the nn lines is expected to be larger in the Gd ESR, the measured shift involves a contribution of those nn sites and is much smaller than that expected for the 1st nn signal.

As for the analysis of the Al NMR data in LASCO, the authors of course do not question the existence of a local moment. But, they still consider that AF correlations are reduced near the impurity, and that the induced moments on the four copper near neighbours are decoupled. Further, they even anticipate that a state nearer to that observed in the overdoped material prevails at distances just greater than the 1st nn distance [13]. However, we feel that there is no experimental evidence for such a possibility in their work on the LASCO system. The only argument advanced by Ishida *et al.* to support this hypothesis is the independent experimental evidence found in their group for two T_1 components in their ^{63}Cu NQR measurements in Zn doped YBCO_7 , and in $\text{YBa}_2\text{Cu}_4\text{O}_8$ [23, 34]. In both cases they find that the long T_1 component is longer than that observed in the pure system, and they therefore associate it with Cu nuclei near the Zn impurities. This leads them to conclude that the magnetic fluctuations near the Zn impurities have been suppressed. However, the relative magnitude of the two components in terms of number of sites and their dependence on Zn doping which could support this interpretation has not been studied in detail. Most importantly, the underlying idea seems to us to contain an essential contradiction. Indeed if the AF fluctuations around the Zn were suppressed, this would imply that Zn is in a classical metallic environment, which would be totally inconsistent with the occurrence of a local moment [32].

In the superconducting state, Ishida *et al.* do find ^{63}Cu NQR relaxation rates much larger than those found in the pure system, which indicates the existence of states in the superconducting gap. This is also seen from Yb Mossbauer experiments on samples in which a small fraction of Y has been substituted by Yb [35]. States in the gap in the superconducting state induced by Zn impurities were also seen by neutron scattering experiments [19]. Those states are found at a scattering vector of (π, π) , even for $\text{YBCO}_7\text{:Zn}$, while a scattering at (π, π) for this oxygen content can hardly be detected in the pure system. These experiments

are thus direct evidences in favor of the persistence of AF correlations in the vicinity of the impurities.

All these observations support the main point which we have been advocating, that the AF correlations are at least maintained, and perhaps even strengthened near the Zn impurities. In such a case the local moment cannot be considered as formed of four independently fluctuating moments on the four Cu sites nn to Zn, but rather as an extended state involving further neighbours, and in which the Cu nn to Zn are ferromagnetically correlated and fluctuate as a single entity.

We therefore think that the experimental observation done by Ishida *et al.* on the normal state ^{63}Cu NQR T_1 might have a quite distinct interpretation. A more systematic study, possibly with different impurities might be needed to clarify the origin of the longer T_1 component.

In conclusion, it seems to us that the existing experiments do not contradict the main point of view originally proposed, *i.e.* that the local moments induced by Zn are associated with the *correlated* nature of the CuO_2 planes and that AF correlations might even actually be enhanced around Zn.

4.5 Induced spin polarisation at large distance from the Zn

Up to now we have mainly considered the magnetic moments induced near the Zn impurities. In noble metals hosts, any local charge perturbation is known to induce long distance charge density oscillations (also called Friedel oscillations). Similarly a local moment induces a long distance oscillatory spin polarisation (RKKY) which has an amplitude which scales with the coupling J_{ex} of the local moment with the conduction electrons. This oscillatory spin polarisation gives a contribution to the NMR shift of the nuclei which decreases with increasing distance from the impurity. In very dilute samples, if the experimental sensitivity is sufficient, the resonances of the different shells of neighbours to the impurity can be resolved [38]. These resonances merge together if the impurity concentration is too large, which results then in a net broadening of the host nuclear resonance.

Here, the occurrence of the local moment, even induced by the non-magnetic substitution is also a local magnetic perturbation in the correlated host. One therefore expects a response which will extend to long distances from the impurity. Such contributions to the NMR linewidths have been found in our work. We shall consider here in turn the case of $\text{YBCO}_{6.6}$ and that of YBCO_7 .

4.5.1 $\text{YBCO}_{6.6}$

Indeed, both the central ^{89}Y line as well as the near neighbour resonances have been found to be broadened in $\text{YBCO}_{6.6}$. As seen in Figures 7 and 9, these linewidths increase at low- T and also increase with increasing impurity content. The central line broadening is unfortunately only a small fraction of the pure compound linewidth, and

the temperature dependence of the impurity induced contribution cannot be extracted accurately. Experiments have therefore been performed by Bobroff *et al.* [27] on ^{17}O nuclei in substituted samples. The larger hyperfine coupling of the ^{17}O nuclei with the planar Cu as compared to that of ^{89}Y lead consequently to broadenings of the ^{17}O NMR width, which have been studied in great detail both for Ni and Zn substitutions. It has been found that in both cases the broadening increases much faster than $1/T$ at low temperatures, contrary to what one might expect in a non-correlated metallic host. This fast increase is a signature of the anomalous magnetic response of the host which displays a peak near the AF wavevector (π, π) .

In the present experiments, the broadenings of the 1st nn line (Fig. 7) are somewhat related to this long distance polarisation induced by the Zn impurity. The large increase of the nn linewidth with increasing Zn concentration is due to the distribution of susceptibility of the moments associated with their mutual interaction. In a molecular field approach, the Curie contribution K_c to the shift of a ^{89}Y nn of a given Zn atom is proportional to $\chi(H_0 + H_m)$, where χ is the single impurity dimensionless susceptibility ($= c_{\text{imp}}/T$) and H_m the molecular field at the moment site induced by other Zn moments. This molecular field scales with the magnetization of the local moments ($H_m = kM$) and therefore varies as $1/T$. The linewidth is then related to the root mean square value of the molecular field δH_m . Consequently, the linewidth due to interaction between the local moments (which scales with $\chi\delta H_m$) should scale as $1/T^2$. We have therefore plotted in Figure 22 the quantity $T^2\Delta H_{\text{corr}}/H$ versus T , where $\Delta H_{\text{corr}} = \Delta H_{\text{nn}} - \Delta H_{\text{pure}}$ is the increase of the nn satellite linewidth (Full Width at Half Maximum) with respect to that of ^{89}Y in pure $\text{YBCO}_{6.6}$. We can see that $T^2\Delta H_{\text{corr}}/H$ is nearly T -independent as expected from such a simple model. Let us point out that H_m should in principle behave as the long distance spin polarisation detected by ^{17}O NMR, and should then increase faster than $1/T$ at low temperature. Although the experimental accuracy on the NMR width is not great, a large increase of $T^2\Delta H_{\text{corr}}/H$ is not observed at low T . More detailed and possibly more accurate experiments are required to better understand whether other contributions to the nn linewidth have to be considered as well.

From our data we can however get an overestimate of δH_m from a comparison of the magnitude of the linewidth with the actual shift of the nn line. Assuming a Gaussian shape for this resonance $\Delta H_{\text{corr}}/2.36$ is simply proportional to $\chi\delta H_m$, while the shift $K_c H_0$ is proportional to χH_0 . Therefore, $\delta H_m = 0.42 \Delta H_{\text{corr}}/K_c$. Further, from the analysis of equation (3), $K_c \simeq 0.024/T$. From the discussion above, $\Delta H_{\text{corr}} = 2.36kc_{\text{imp}}^2 H_0/T^2$ and from Figure 22 for 1% Zn, $\Delta H_{\text{corr}} \simeq 2H_0/T^2$. Then, for an applied field $H_0 = 7$ Tesla, we deduce

$$\delta H_m = 250/T(\text{Tesla}/\% \text{Zn}). \quad (13)$$

The molecular field becomes comparable with the thermal energy for $k_B T = \mu_{\text{eff}} H_m$, which for a measured $\mu_{\text{eff}} \simeq 0.8\mu_B$ in $\text{YBCO}_{6.6}$ corresponds to about 1.2 Tesla/K.

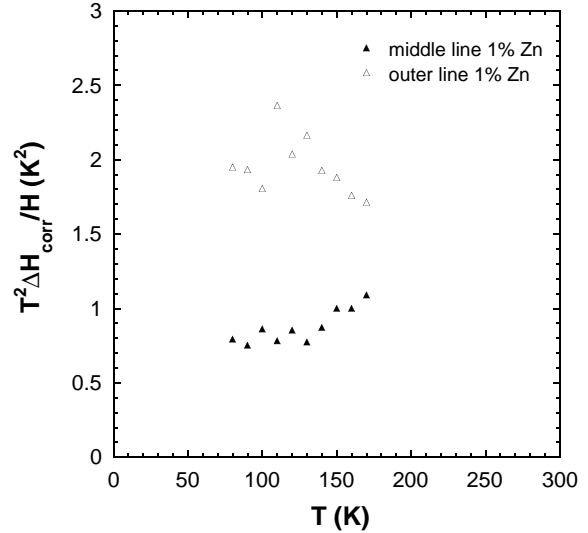


Fig. 22. Variation of the product of the square of temperature T^2 and the nn linewidth ΔH_{corr} (linewidth of the pure compound has been subtracted from the measured linewidth) with the temperature T for $\text{YBCO}_{6.64}:\text{Zn}$.

Therefore the temperature at which a spin-glass freezing of this system should occur can be estimated to be about 15 K for 1% Zn. This number deduced from this rough analysis is somewhat higher than that obtained from the Weiss temperature measured by static susceptibility by Mendels *et al.* [9], which does not exceed 4 K for 4% Zn. Apart from the above mentioned possible experimental limitations, this difference could be linked with the fact that we are dealing here with a 2D Heisenberg spin system, for which quantum fluctuations reduce the spin-glass ordering temperature to $T_g = 0$ [36]. A finite value for T_g would then only result from weak interplane exchange couplings.

4.5.2 YBCO_7

The broadening has been found to increase as $1/T$ at low- T , for this slightly overdoped composition for which the planar susceptibility of the pure system has little T -dependence. This increased linewidth at low- T is a direct proof of the existence of a local moment behaviour induced by Zn for this overdoped system [38]. We have seen that the absence of near neighbour resonance lines is also an indication that the effective moment is very small, which confirms the susceptibility data of Mendels *et al.* A similar observation has been made by Bobroff *et al.* [27] through ^{17}O NMR data. Initially such a broadening can be explained with the RKKY-like broadening induced by the local moments. However, in the underdoped case it has been shown that the response of the correlated electronic system is quite distinct from that of a free electron gas, as the ^{17}O NMR linewidth exhibits an anomalous T dependence. The NMR data for the YBCO_7 composition, both for ^{17}O and ^{89}Y , does not display such an anomalous T -dependence, and one might wonder whether

a conventional RKKY broadening is then recovered. Such an approach has been used in our initial report [8]. However, the very fact that a T -dependent magnetic behaviour is induced by Zn substitution is an indication that *the correlated nature of the electronic state has not disappeared in YBCO₇*. This is also established by the well known anomalous non-Korringa T -dependence of ^{63}Cu [37]. Therefore a direct test of the shape of the spatial dependence of the impurity induced spin polarisation should give us information on the importance of these correlations. This aim will be pursued in the future with careful studies of the NMR lineshapes, which are expected to be more sensitive to the detailed shape of the spin polarisation [27]. Such experimental studies will be undertaken on ^{17}O NMR which possesses a larger signal to noise ratio. A comparative discussion of the induced spin polarisation as sensed by the ^{89}Y and the ^{17}O nuclei will therefore be performed in the future.

5 Conclusions

A large variety of conclusions have been drawn and various questions have been raised from the present results. They address different points extending from the materials properties to detailed questions on the electronic structure of the impurities and their influence on superconductivity.

First, concerning the *physical chemistry* of the cuprates, the intensity of the near neighbour resonances allowed us to calibrate the amount of Zn substituted on the planar Cu sites. Our result is the strongest experimental proof that the Zn substitutes dominantly on this planar site, up to 3% Zn, and within 10% experimental accuracy.

We have confirmed the influence of Zn impurities on the *phase diagram* of the cuprates in the underdoped regime. The implication that the static and dynamic susceptibility far from the impurity is unaffected by Zn is borne out by our shift and relaxation data. This demonstrates that the related $\mathbf{q} = 0$ pseudo-gap is not modified. The change of the macroscopic susceptibility is only associated with modifications of magnetic properties in the vicinity of the impurity. Kakurai *et al.* [18] initially suggested, on the basis of their neutron scattering experiments, that the pseudo-gap vanishes at $\mathbf{q} = (\pi, \pi)$ while the gap at other \mathbf{q} values is unchanged. However, the neutron data of Sidis *et al.* [19] in fact suggests that the pseudo-gap at $\mathbf{q} = (\pi, \pi)$ does not vanish but that some states appear in the pseudo-gap. Those could also be associated with the local magnetic modifications induced around the Zn. In a scenario in which the pseudo gaps would be associated with the formation of local pairs at high- T , these results indicate that impurities do not prevent the formation of local pairs except possibly in their vicinity.

What are the actual magnetic properties *in the vicinity of the Zn impurity*? Although our early experiments had given strong proofs of the occurrence of a local moment behaviour induced by non-magnetic Zn impurities, the validity of this observation has been periodically put into question. The significance of the nn

^{89}Y NMR results has been, for instance, questioned from the absence of detectable nn resonances of Zn in the ESR experiments on Gd/Y substituted underdoped samples. We have clearly shown here that the large expected relaxation rate induces a broadening of the Gd ESR nn lines which prohibits their detection. The authors have also concluded from those Gd ESR experiments that the full density of states corresponding to pure YBCO₇ is restored near the Zn impurity. The fact that the ^{89}Y 1st nn resonance is found to display an NMR shift much larger than that of the optimally doped compound at low- T , is clear evidence against this idea. On the contrary, the susceptibility of the Cu nn to Zn is found to present a Curie like T -dependence, hence the “local moment” denomination, which we have been using throughout. This local moment behaviour is confirmed in YBCO_{6.6} by macroscopic susceptibility SQUID data [9,16].

It is clear that the observed local moment behaviour is original inasmuch as it is the *magnetic response of the correlated electron system to the presence of a spinless site*. The perturbation induced by Zn extends at least to the four nn copper sites, but we have shown that, in underdoped YBCO_{6.6}, our data are compatible with a local dynamic AF state which extends over more Cu sites. Although the present NMR data are not sufficient to allow us to determine the actual extension of this state, the width of the neutron scattering peak at (π, π) which is found to develop at low- T within the pseudo-gap in presence of Zn [19], corresponds to a real space extension of at least 7 Å.

Various theoretical arguments in favor of the *occurrence of a local moment in presence of a spinless site in a correlated electronic system* have been advanced [6,39–41]. As complete understanding of the magnetic properties of pure cuprates is far from being achieved, it is no surprise that the present theoretical descriptions of the impurity induced magnetism are rather crude and, for example, do not address its microscopic extent. Our results might, however, be put in parallel with recent theoretical work on undoped quantum spin systems. For instance Martins [42] predicts static local moments induced due to doping $S = 1/2$ Heisenberg AF chains or ladders with non-magnetic impurities. NMR experiments on the $S = 1/2$ Heisenberg chain system Sr_2CuO_3 are consistent with the prediction of an induced local moment with a large spatial extent along the chain [43]. In this undoped insulating quantum liquid, the response is then purely magnetic. Since the parent compound to YBCO superconductors is a 2D Heisenberg AF and dynamic AF correlations appear to persist even in the metallic compositions, appearance of local moments on many Cu sites near to the doped Zn might well be anticipated.

In the slightly overdoped YBCO₇, the local moment could initially only be detected through the induced long distance spin polarisation [7]. A local moment induced by non-magnetic Al substituted on Cu is also detected in optimally doped LSCO from ^{27}Al NMR. The fact that we could not resolve the nn signal in YBCO₇

is consistent with the weak magnitude found for the Curie like contribution to the local susceptibility. The *decreasing magnitude of the moment with increasing hole doping* could carefully be monitored by direct SQUID measurements [16]. This decrease could be linked experimentally with a *decreasing screening radius* by the conduction band. However, the magnetic states which are detected within the spin-gap at low- T by neutron scattering [19] exhibit a short magnetic correlation length, so that the spatial extent of the local moment also decreases with increasing hole doping as does the AF correlation length in the pure system. Altogether, our experiments cannot, at present, distinguish the *respective roles of the screening radius and the AF correlation length in defining the local moment magnitude and spatial extent*.

Another important question which arises then concerns the *coupling of the defect local moment to the host*. For magnetic impurities in simple metals, an exchange coupling J_{ex} between the local moment and the conduction electron spins usually occurs, and determines some of the thermodynamic properties of the local moment. For instance the *fluctuation rate of the local moment* ($1/\tau$) is directly determined by J_{ex} , and follows a Korringa relation in classical metals. This fluctuation time can be estimated from nuclear spin lattice relaxation data. In the YBCO system we could only obtain such measurements in the underdoped regime on the ^{89}Y nn of Zn. From these we could show that only weak contributions to $1/T_1$ are expected on the ^{89}Y nn in the optimally doped case, and could not be sensed within experimental accuracy. Direct measurements of the ^{27}Al T_1 are on the contrary sensitive enough in the optimally doped case in LASCO, as seen by Ishida *et al.* Their results, although they establish the occurrence of a local moment induced by the spin-less Al^{3+} substituent, differ markedly from those obtained in YBCO. A large temperature independent contribution to the shift and local moment fluctuation time is detected, contrary to our observations. The origin of the difference might be:

- i) linked with the larger valence of Al^{3+} , *i.e.* the charge difference with respect to host planar Cu^{2+} ;
- ii) a peculiarity of the LASCO system, as indeed the physical properties of this system do not appear to fit in a universal picture with the other cuprates (see Ref. [44]);
- iii) or merely a difference between underdoped and optimally doped systems, as the experiments could not be performed on the two systems under similar conditions.

Further experiments will certainly permit to make a decision between these possibilities. Currently, experiments do not permit a clear indication on the applicability of an exchange model. In conventional metallic systems, the local moment couples through J_{ex} to the electron bath and an oscillatory RKKY polarization occurs in the band. Therefore J_{ex} can be usually estimated from the broadening of the host NMR [24,45]. Applying the standard RKKY theory yields values of the exchange coupling which are very large [8]. But, we have recently shown in

Orsay [27] that, at least in the underdoped regime, the behaviour of the ^{17}O linewidth does not follow the expected RKKY T -dependence at all, *i.e.* the NMR width does not scale solely with the impurity magnetization. Let us note here that whatever the method used [8,13], the estimates of the coupling constant are presently such that if one applies a simple exchange model, one would expect a *large Kondo temperature* T_K and correspondingly, a spin susceptibility which would deviate from the Curie dependence at $T \sim T_K$ and saturate below. From SQUID data, Mendels *et al.* concluded that this is not the case, and that T_K does not exceed at most a few K, in the underdoped YBCO compounds. Such a Kondo-like effect was a candidate mechanism for the reduction of the magnitude of the local moment in $\text{YBCO}_{7:\text{Zn}}$ (see for instance Ref. [46]). But obviously the Kondo model needs to be revised in the context of a strongly correlated electron system. Such difficulties had been already pointed out by Hirschfeld [47] in view of our preliminary experimental results.

In conclusion, we have detailed here the experimental evidence for the occurrence of a local moment behaviour induced by spinless substitutions on the Cu site in CuO_2 planes of cuprates. The existence of original magnetic behaviour induced by non-magnetic substitutions can be anticipated from current theoretical treatments of *undoped* low-dimensional spin systems. However, the detailed experimental observations reported here on *doped* cuprates do not have a thorough interpretation from the theoretical standpoint. We suggest that further experimental and theoretical efforts regarding these properties are essential to lead us towards a comprehensive description of the magnetic and superconducting properties of the cuprates.

We would like to thank P. Mendels, J. Bobroff, and A. Macfarlane for useful discussions and comments about the manuscript. Laboratoire de Physique des Solides is a "Unité Mixte de Recherches du Centre National de la Recherche Scientifique et de l'Université Paris-Sud".

References

1. H. Alloul, T. Ohno, P. Mendels, Phys. Rev. Lett. **63**, 1700 (1989).
2. W.W. Warren *et al.*, Phys. Rev. Lett. **62**, 1193 (1989); M. Horvatic *et al.*, Phys. Rev. B **39**, 7322 (1989).
3. C. Berthier *et al.*, Appl. Magn. Reson. **3**, 449 (1992).
4. J. Rossat-Mignod *et al.*, Physica C **185-189**, 86 (1991).
5. R. Birgeneau, in *Physical Properties of High T_c Superconductors*, edited by D.M. Ginsberg (World Scientific, Singapore, 1989), vol. I.
6. A.M. Finkelstein, V.E. Kataev, E.F. Kukovitskii, G. B. Teitelbaum, Physica (Amsterdam) C **168**, 370 (1990).
7. H. Alloul, P. Mendels, H. Casalta, J.F. Marucco, J. Arabski, Phys. Rev. Lett. **67**, 3140 (1991).

8. A.V. Mahajan, H. Alloul, G. Collin, J.F. Marucco, *Phys. Rev. Lett.* **72**, 3100 (1994).
9. P. Mendels, J. Bobroff, G. Collin, H. Alloul, M. Gabay, J. F. Marucco, N. Blanchard, B. Grenier, (submitted to *Europhys. Lett.*).
10. R. Dupree, A. Gencten, D. McK. Paul, *Physica C* **193**, 193 (1992) and references therein.
11. R.E. Walstedt, R.F. Bell, L.F. Schneemeyer, J.V. Waszczak, W.W. Warren, R. Dupree, A. Gencten, *Phys. Rev. B* **48**, 10646 (1993).
12. G.V.M. Williams, J.L. Tallon, R. Meinhold, A. Janossy, *Phys. Rev. B* **51**, 16503 (1995).
13. K. Ishida, Y. Kitaoka, K. Yamazoe, K. Asayama, Y. Yamada, *Phys. Rev. Lett.* **76**, 531 (1996).
14. A. Janossy, J.R. Cooper, L.C. Brunel, A. Carrington, *Phys. Rev. B* **50**, 3442 (1994).
15. J.R. Cooper, *Supercond. Sci. Technol.* **4**, S181 (1991).
16. P. Mendels, H. Alloul, J.H. Brewer, G.D. Morris, T.L. Duty, S. Johnston, E.J. Ansaldo, G. Collin, J.F. Marucco, C. Niedermayer, D. R. Noakes, C.E. Stronach, *Phys. Rev. B* **49**, 10035 (1994).
17. S. Shamoto, T. Kiyokura, H. Harashina, M. Sato, *J. Phys. Soc. Jpn* **63**, 2324 (1994).
18. K. Kakurai, S. Shamoto, T. Kiyokura, M. Sato, J.M. Tranquada, G. Shirane, *Phys. Rev. B* **48**, 3485 (1993).
19. P. Bourges, Y. Sidis, B. Hennion, R. Villeneuve, J.F. Marucco, G. Collin, *Czech. J. Phys. France* **46**, 1155 (1996); P. Bourges, Y. Sidis, L.P. Regnault, B. Hennion, R. Villeneuve, G. Collin, C. Vettier, J.Y. Henri, J.F. Marucco, *J. Phys. Chem. Solids* **56**, 1937 (1995); Y. Sidis *et al.*, *Int. J. Mod. Phys. B*, (to be published).
20. T.R. Chien, Z.Z. Wang, N.P. Ong, *Phys. Rev. Lett.* **67**, 2088 (1991).
21. K. Mizuhashi, K. Takenaka, Y. Fukuzumi, S. Uchida, *Phys. Rev. B* **52**, R3884 (1995).
22. J.W. Loram, K.A. Mirza, P.F. Freeman, *Physica (Amsterdam) C* **171**, 243 (1990).
23. K. Ishida, Y. Kitaoka, N. Ogata, T. Kamino, K. Asayama, J.R. Cooper, N. Athanassopoulou, *J. Phys. Soc. Jpn* **62**, 2803 (1993).
24. H. Alloul, T. Ohno, H. Casalta, J.F. Marucco, P. Mendels, J. Arabski, G. Collin, M. Mehbod, *Physica C* **171**, 419 (1990).
25. L. Guerrin, H. Alloul, G. Collin, *Physica C* **251**, 219 (1995).
26. A. Lanckbeen, C. Legros, J.F. Marucco, R. Deltour, *Physica C* **221**, 53 (1994); G. Collin, (private communication).
27. J. Bobroff, H. Alloul, Y. Yoshinari, P. Mendels, A. Keren, N. Blanchard, G. Collin, J.F. Marucco, *Phys. Rev. Lett.* **79**, 2117 (1997).
28. G.V.M. Williams, J.L. Tallon, R. Meinhold, *Phys. Rev. B* **52**, R7034 (1995).
29. M. Takigawa, P.C. Hammel, R.H. Heffner, Z. Fisk, K.C. Ott, J.D. Thompson, *Phys. Rev. Lett.* **63**, 1865 (1989).
30. T. Moriya, *J. Phys. Soc. Jpn* **18**, 516 (1963).
31. S. Zagoulaev, P. Monod, J. Jegoudez, *Phys. Rev. B* **52**, 10474 (1995).
32. H. Alloul, J. Bobroff, P. Mendels, *Phys. Rev. Lett.* **78**, 2494 (1997).
33. Y. Yoshinari *et al.*, Unpublished.
34. G. Zheng, T. Odaguchi, T. Mito, Y. Kitaoka, K. Asayama, Y. Kodama, *J. Phys. Soc. Jpn* **62**, 2591 (1993).
35. J.A. Hodges, P. Bonville, P. Imbert, A. Pinatel-Philippot, *Physica C* **323**, 246 (1995).
36. C. Dekker, A.F.M. Arts, H.W. de Wijn, *Phys. Rev. Lett.* **38** 8985 (1988); C. Dekker, A.F.M. Arts, H.W. de Wijn, A.J. van Duynveldt, J.A. Mydosh, *Phys. Rev. B* **61**, 1780 (1988).
37. M. Takigawa, A.P. Reyes, P.C. Hammel, J.D. Thompson, R.H. Heffner, Z. Fisk, K.C. Ott, *Phys. Rev. B* **43**, 247 (1991).
38. J.B. Boyce, C.P. Slichter, *Phys. Rev. Lett.* **32**, 61 (1974); H. Alloul, F. Hippert, H. Ishii, *J. Phys. F* **4**, 725 (1979) and references therein.
39. N. Nagaosa, T.-K. Ng, *Phys. Rev. B* **51**, 15588 (1995).
40. D. Poilblanc, D.J. Scalapino, Hanke, *Phys. Rev. Lett.* **72**, 884 (1994); see also *Phys. Rev. B* **50**, 13020 (1994).
41. G. Khaliullin, R. Killian, S. Krivenko, P. Fulde, *Physica C* **282-287**, 1749 (1997).
42. G.B. Martins, M. Laukamp, J. Riera, E. Dagotto, *Phys. Rev. Lett.* **78**, 3563 (1997).
43. M. Takigawa, N. Motoyama, H. Eisaki, S. Uchida, *Phys. Rev. B* **55**, 14129 (1997).
44. J. Bobroff, H. Alloul, P. Mendels, V. Viallet, J.F. Marucco, D. Colson, *Phys. Rev. Lett.* **78**, 3757 (1997).
45. R.E. Walstedt, L.R. Walker, *Phys. Rev. B* **9**, 4857 (1974).
46. A. Nagaosa, P. Lee, *Phys. Rev. Lett.* **79**, 3755 (1997).
47. L.S. Borkowski, P.J. Hirschfeld, *Phys. Rev. B* **49**, 15404 (1994).